Strategies for Recognition of Stem-loop RNA Structures by Synthetic Ligands: Application to the HIV-1 Frameshift Stimulatory Sequence

Supplementary Information

*Prakash B. Palde[‡], Leslie O. Ofori[§], Peter C. Gareiss[‡], Jaclyn Lerea[†] and Benjamin L. Miller[†,‡,]**

[†]Department of Dermatology, [‡]Department of Biochemistry and Biophysics, and [§]Department of Chemistry, University of Rochester, Rochester, New York 14642.

Benjamin_Miller@urmc.rochester.edu

Materials and general methods	S2
Spectral data for compounds **2 - 8**	S3-S16
HPLC data for compounds **9** and **10**	S17
Spectral data for compounds **9** and **10**	S18-S26
Assignment of *E* (**9**) and *Z* (**10**) isomers by analogy	S27
Selected fluorescence binding data for compounds **1 - 11**	S28-S32
Filter binding assay for compounds **1** and **5**	S31
Protocol for binding studies using SPR	S33-S34
SPR data for compounds **1** and **9-11**	S35-S38
Dynamic light scattering (DLS) measurements for compounds **9-11**	S39

Materials and General Methods:

Commercially available reagents were obtained from Aldrich Chemical Co. (St. Louis, MO), Fluka Chemical Corp. (Milwaukee, WI), and TCI America (Portland, OR) and used as received unless otherwise noted. Water used for reactions and aqueous work-up was deionized and glass distilled. Reagent grade solvents were used for all non-aqueous extractions. Reactions were monitored by analytical thin-layer chromatography using EM silica gel 60 F-254 pre-coated glass plates (0.25 mm). Compounds were visualized on the TLC plates with a UV lamp (λ = 254 nm) and staining with I_2/SiO_2. Synthesized compounds were purified using flash chromatography on EM silica gel 60 (230-400) mesh.

Analysis:

^{1}H NMR spectra were recorded at 25 °C on a Bruker Avance 400 (400 MHz) and Bruker Avance 500 (500 MHz) instrument. Chemical shifts (δ) are reported in parts per million (ppm) downfield from tetramethylsilane and referenced to residual protium signal in the NMR solvent ($CDCl_3$, δ = 7.26). Data are reported as follows: chemical shift, multiplicity (s = singlet, d = doublet, t = triplet, m = multiplet), integration, and coupling constant (J) in Hertz (Hz). ^{13}C NMR spectra were recorded at 25 °C on a Bruker Avance 400 (100 MHz) or Bruker Avance 500 (125 MHz). Chemical shifts (δ) are reported in parts per million (ppm) downfield from tetramethylsilane and referenced to carbon resonances in the NMR solvent. High resolution mass spectra (HRMS) were acquired either at the University of Buffalo Mass spectrometry facility, Buffalo, New York or from the University of California, Riverside, CA, mass spectrometry facility.

For detailed information on compound **1** including synthesis and spectra characterization, please refer to McNaughton *et al J. Am. Chem. Soc.*, **2007**, *129*, 11306–11307 (**DOI:** 10.1021/ja072114h)

Compound 2, ^{1}H NMR

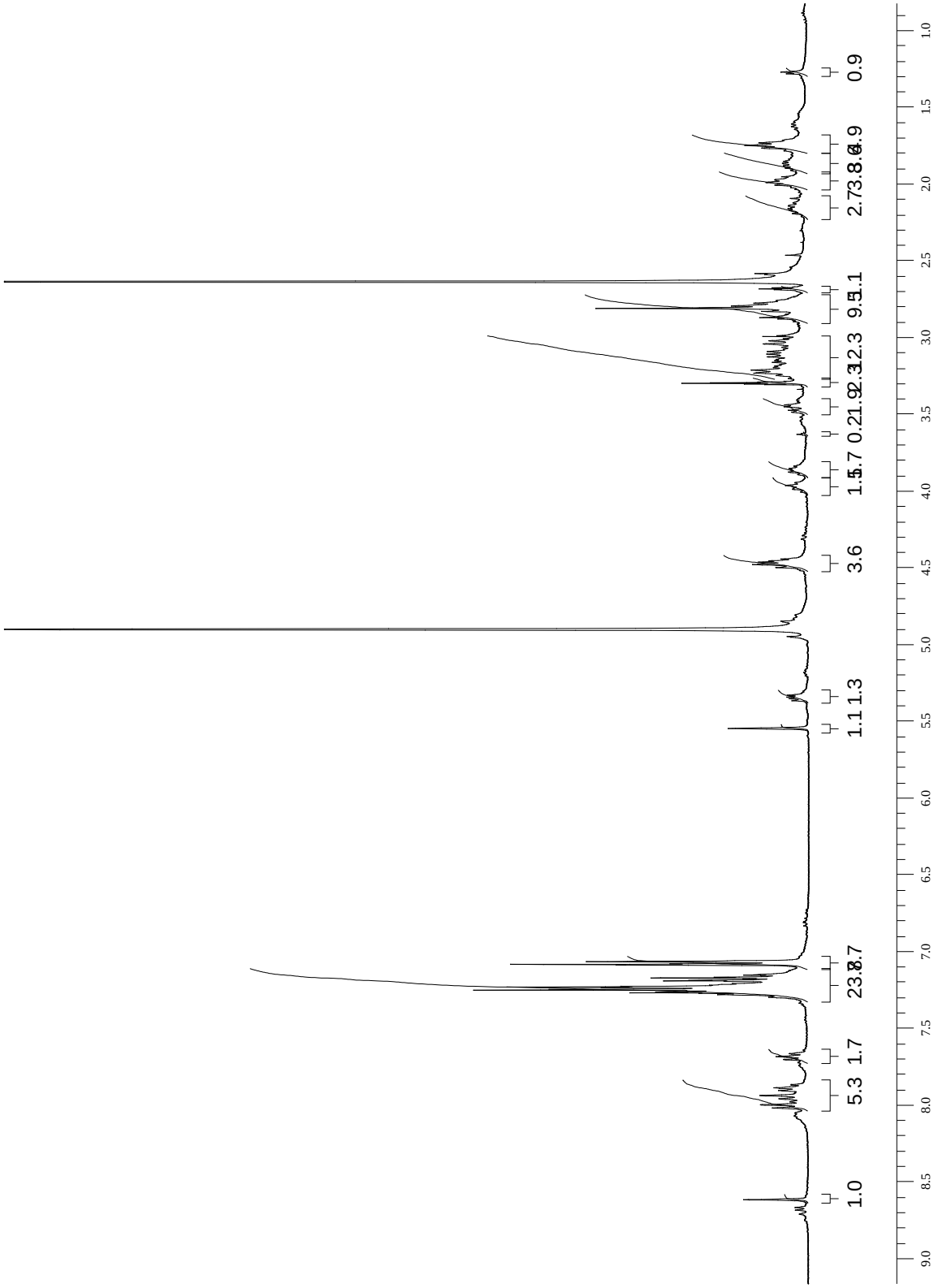

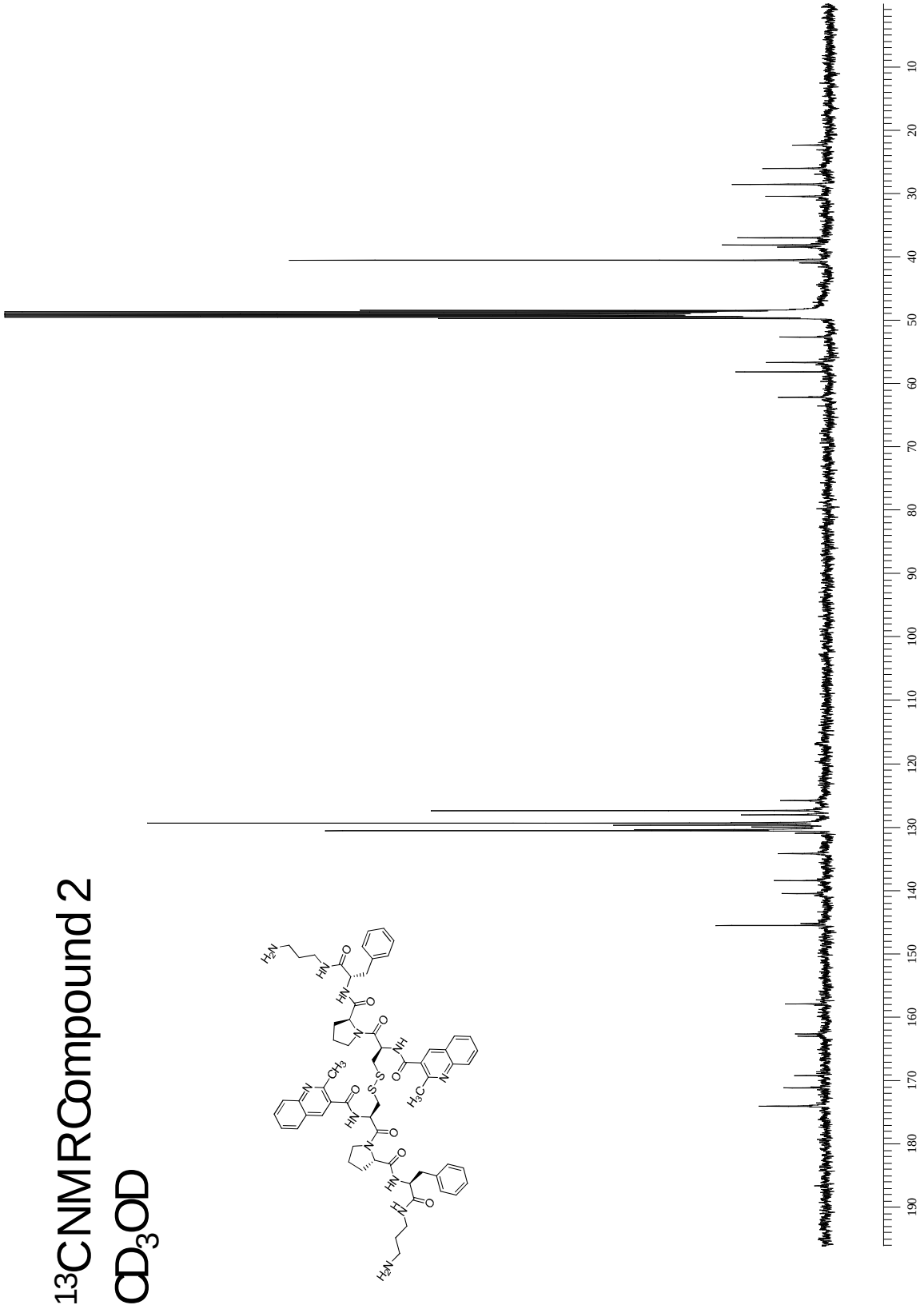
^{13}C NMR Compound 2
CD$_3$OD

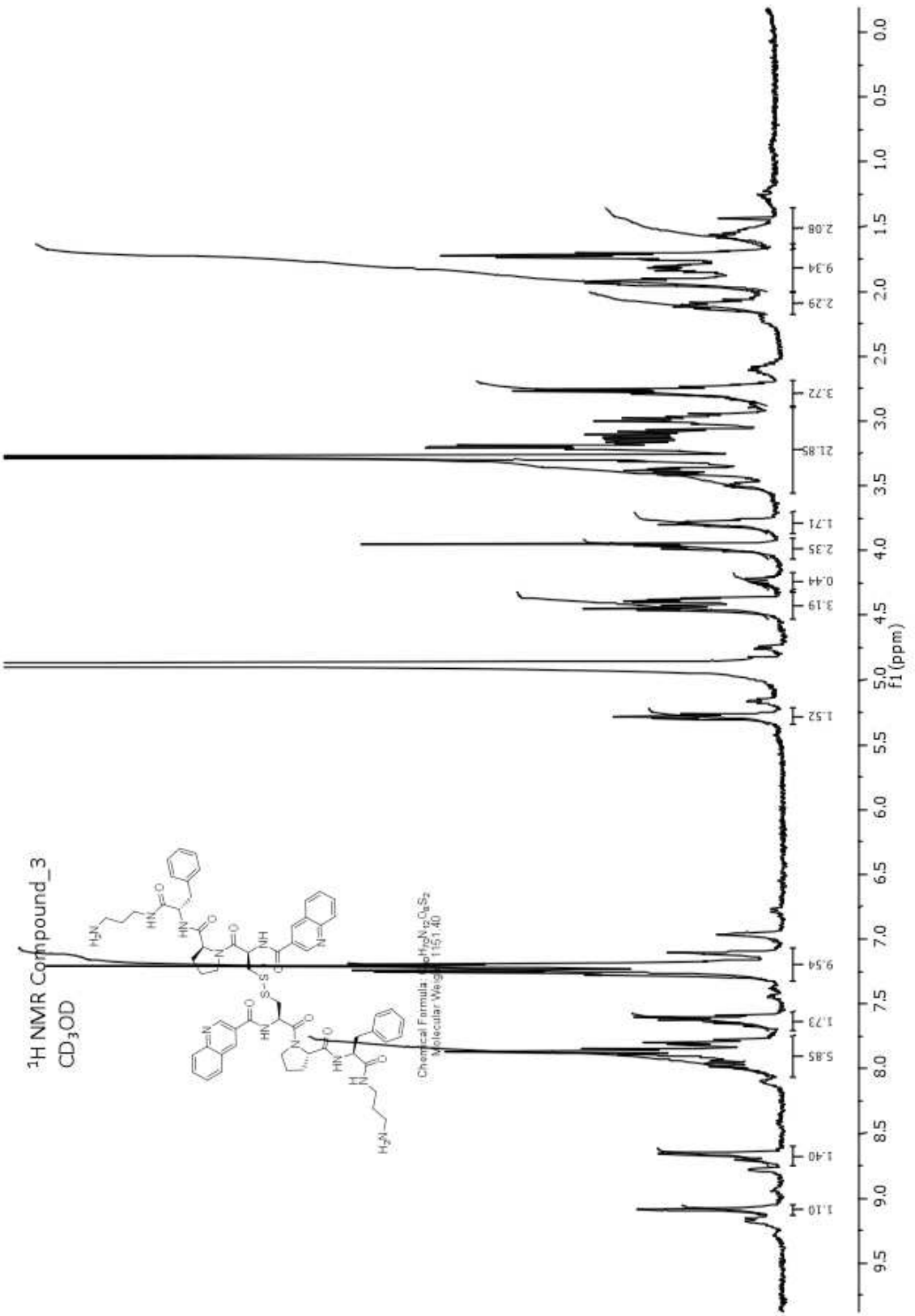
^{1}H NMR Compound_3
CD_3OD
Chemical Formula: $C_{76}H_{92}N_{12}O_6S_2$
Molecular Weight: 1151.40
f1 (ppm)
1.10
1.40
5.85
1.73
9.54
1.52
3.19
0.44
2.35
1.71
21.85
3.22
2.29
9.34
2.08

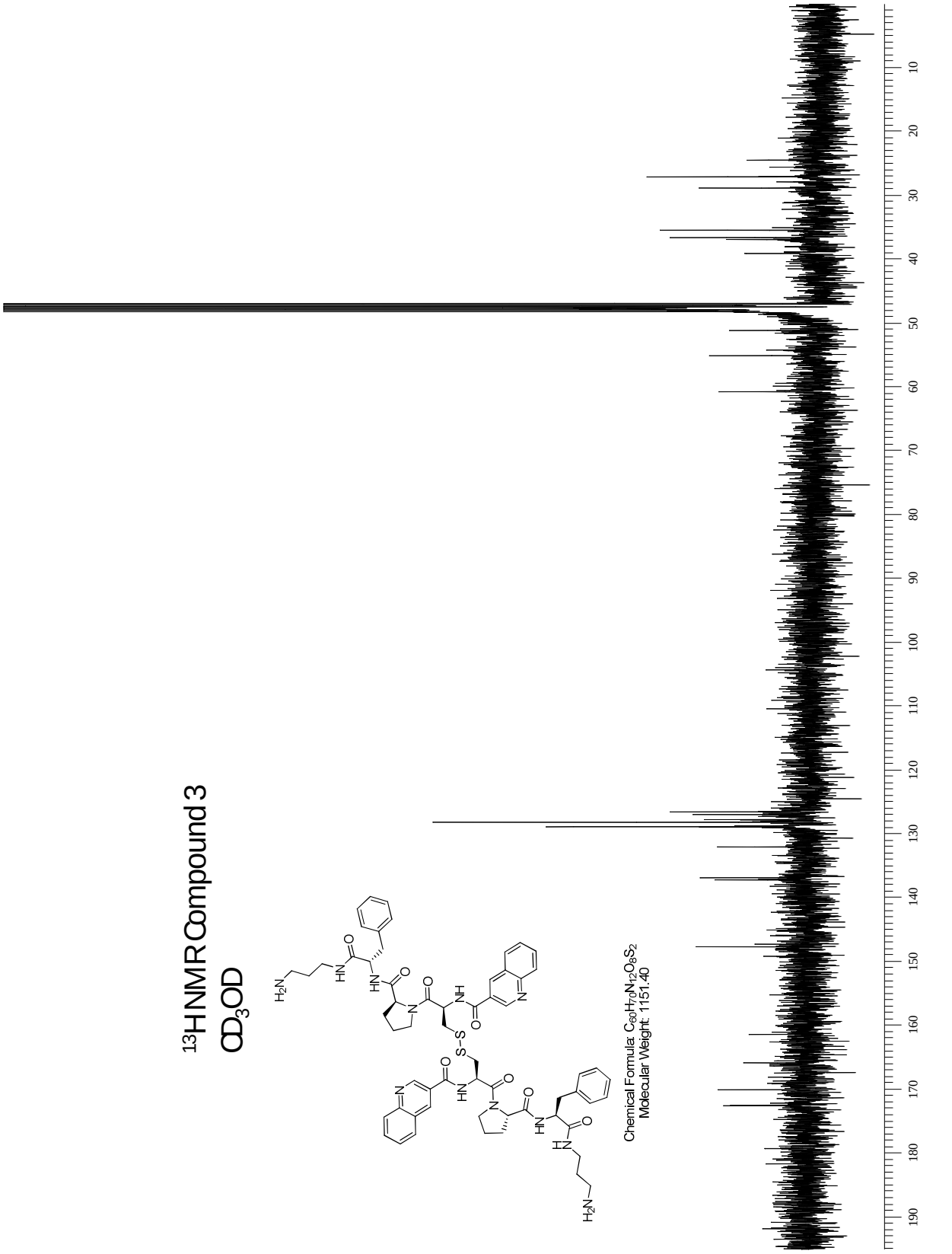
^{13}H NMR Compound 3
CD$_3$OD
Chemical Formula: $C_{68}H_{70}N_{12}O_8S_2$
Molecular Weight: 1151.40

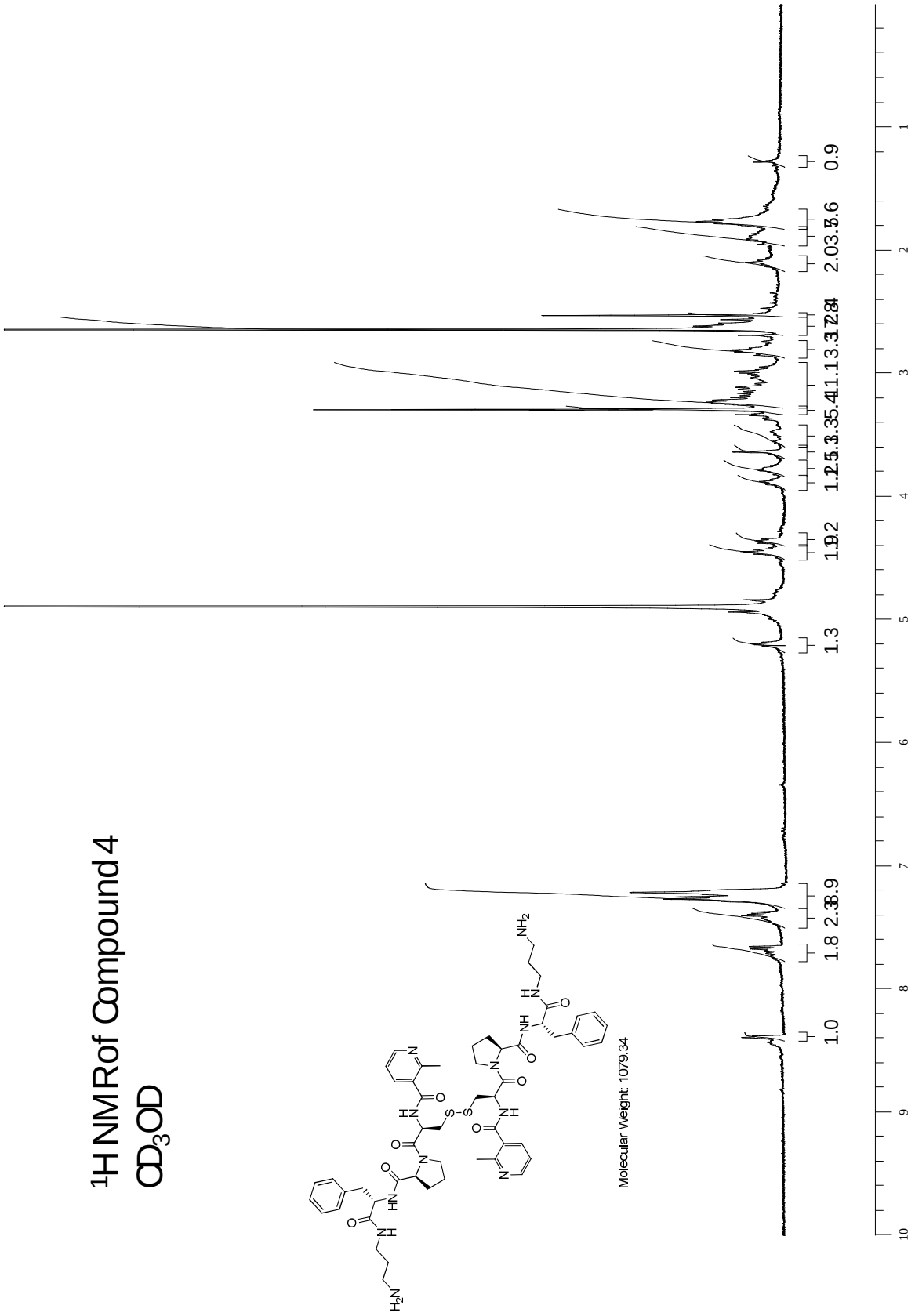
^{1}H NMR of Compound 4
CD_3OD
Molecular Weight: 1079.34
1.0
1.8
2.3
3.9
1.3
1.9
2.0
1.2
5.3
3.3
5.4
1.1
1.3
3.1
2.8
4
2.0
3.5
3.6
0.9

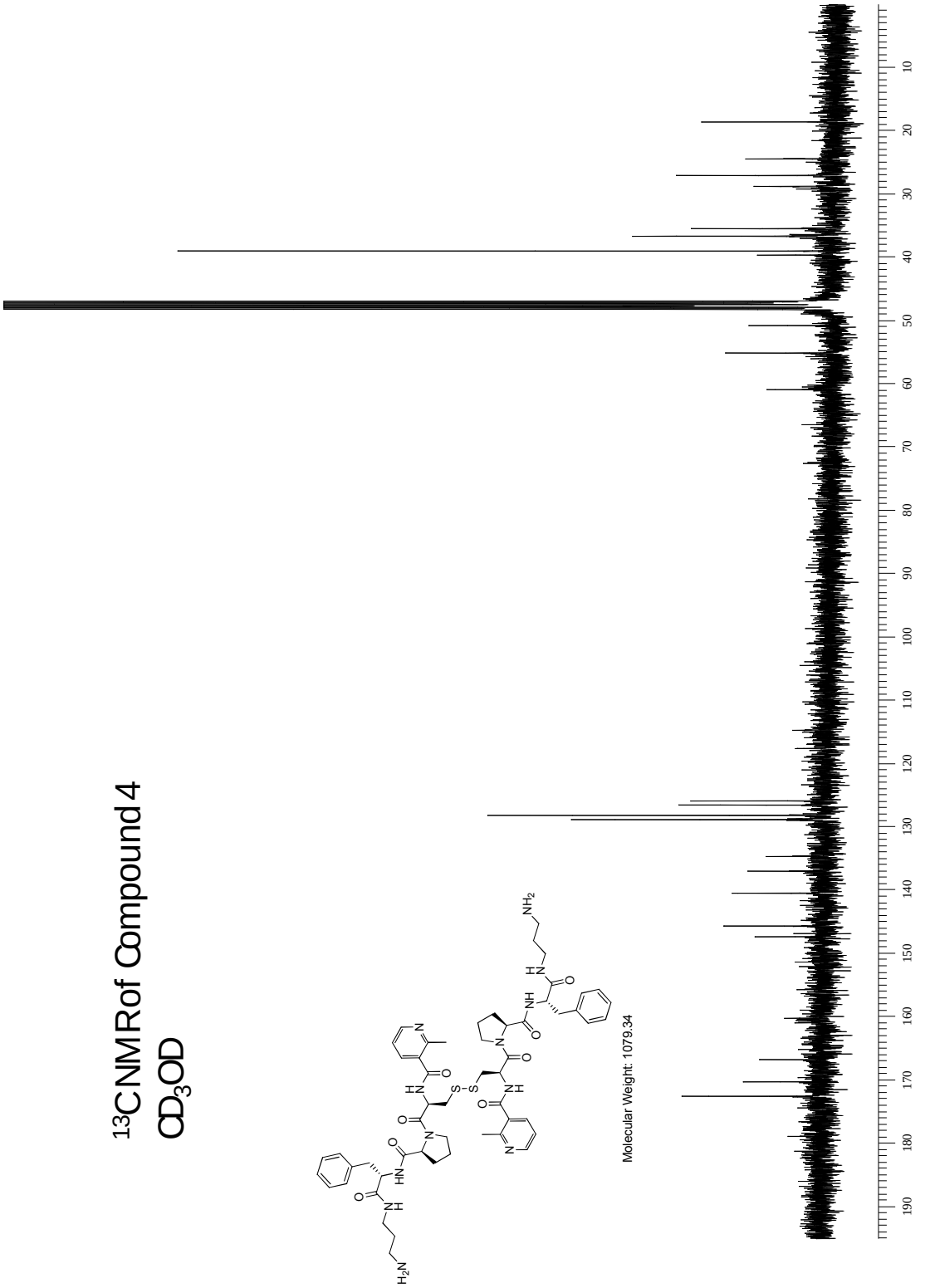
^{13}CNMRof Compound 4
CD_3OD
Molecular Weight: 1079.34

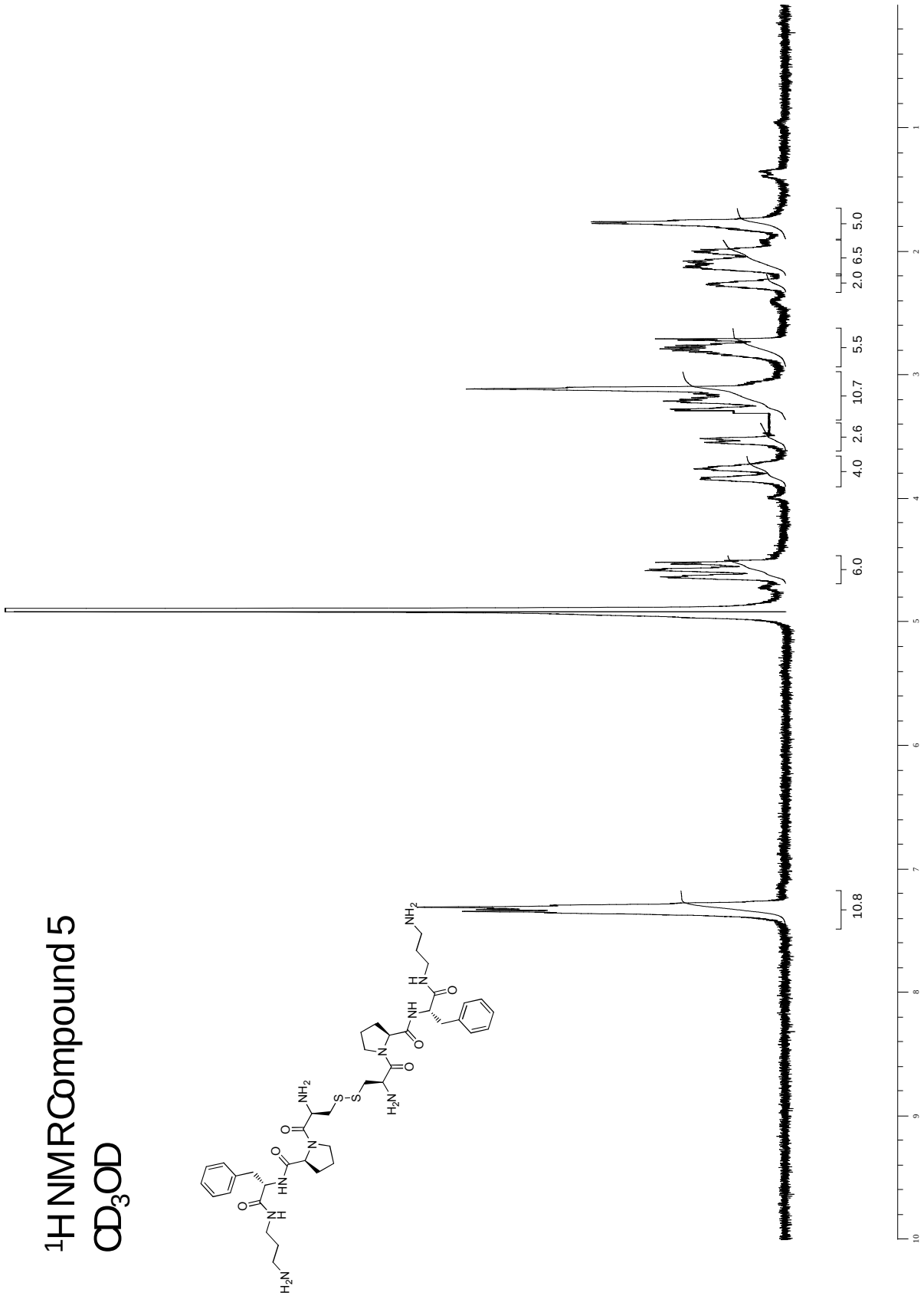
^{1}H NMR Compound 5
CD_3OD
10.8
6.0
4.0
2.6
10.7
5.5
2.0
6.5
5.0

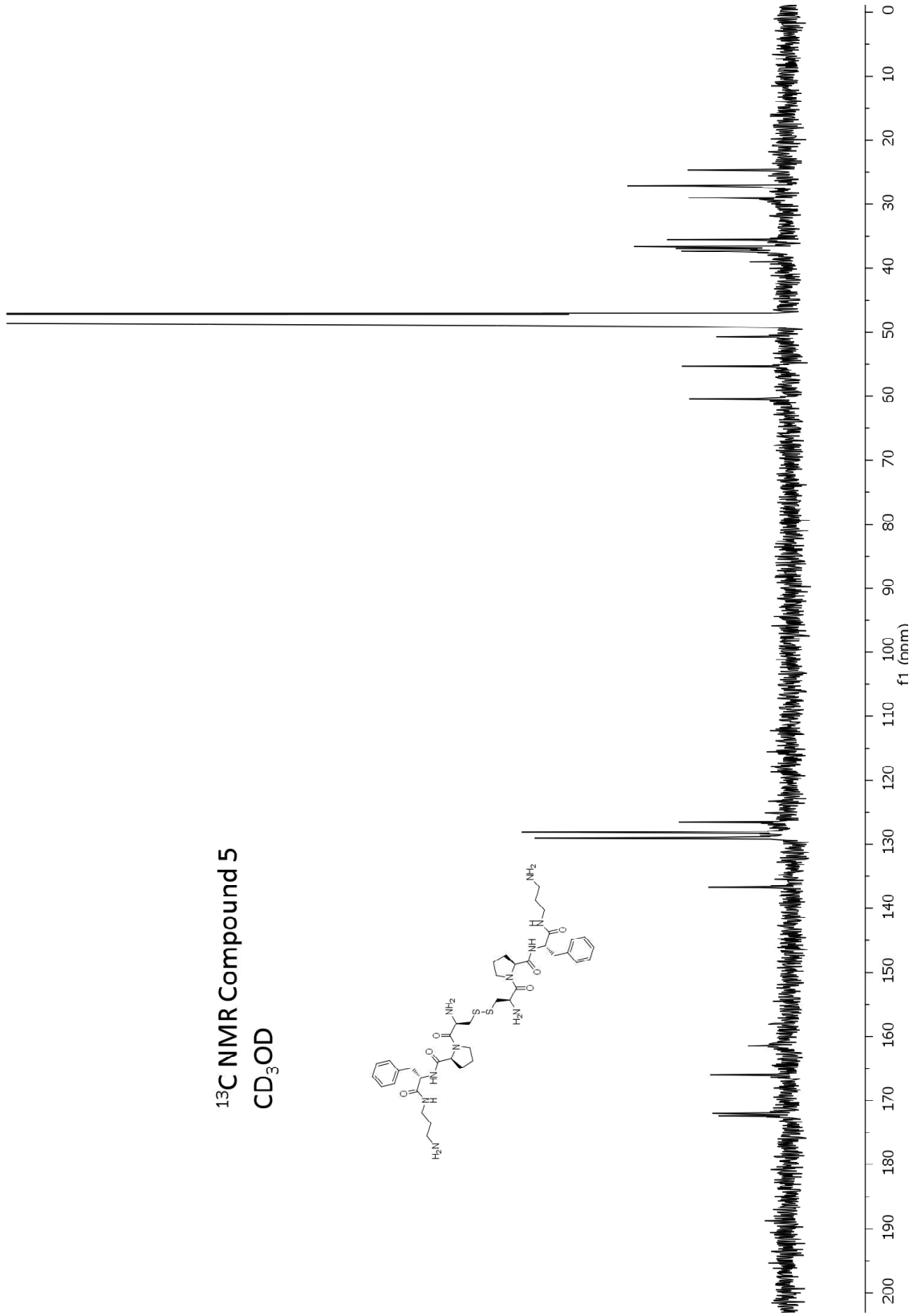
^{13}C NMR Compound 5
CD_3OD
f1 (ppm)

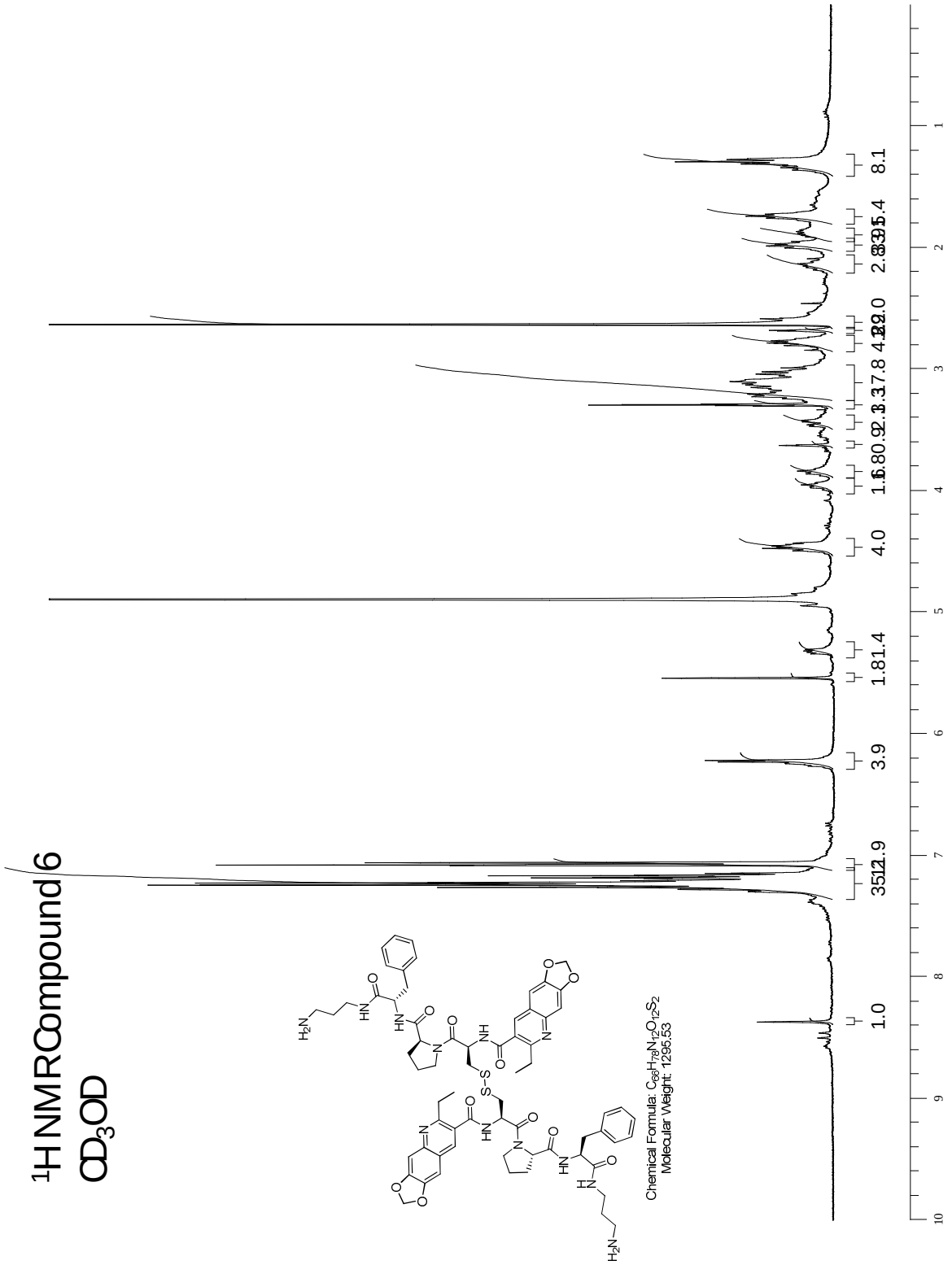
^{1}H NMR Compound 6
CD_3OD
Chemical Formula: $C_{68}H_{78}N_{12}O_{12}S_2$
Molecular Weight: 1295.53

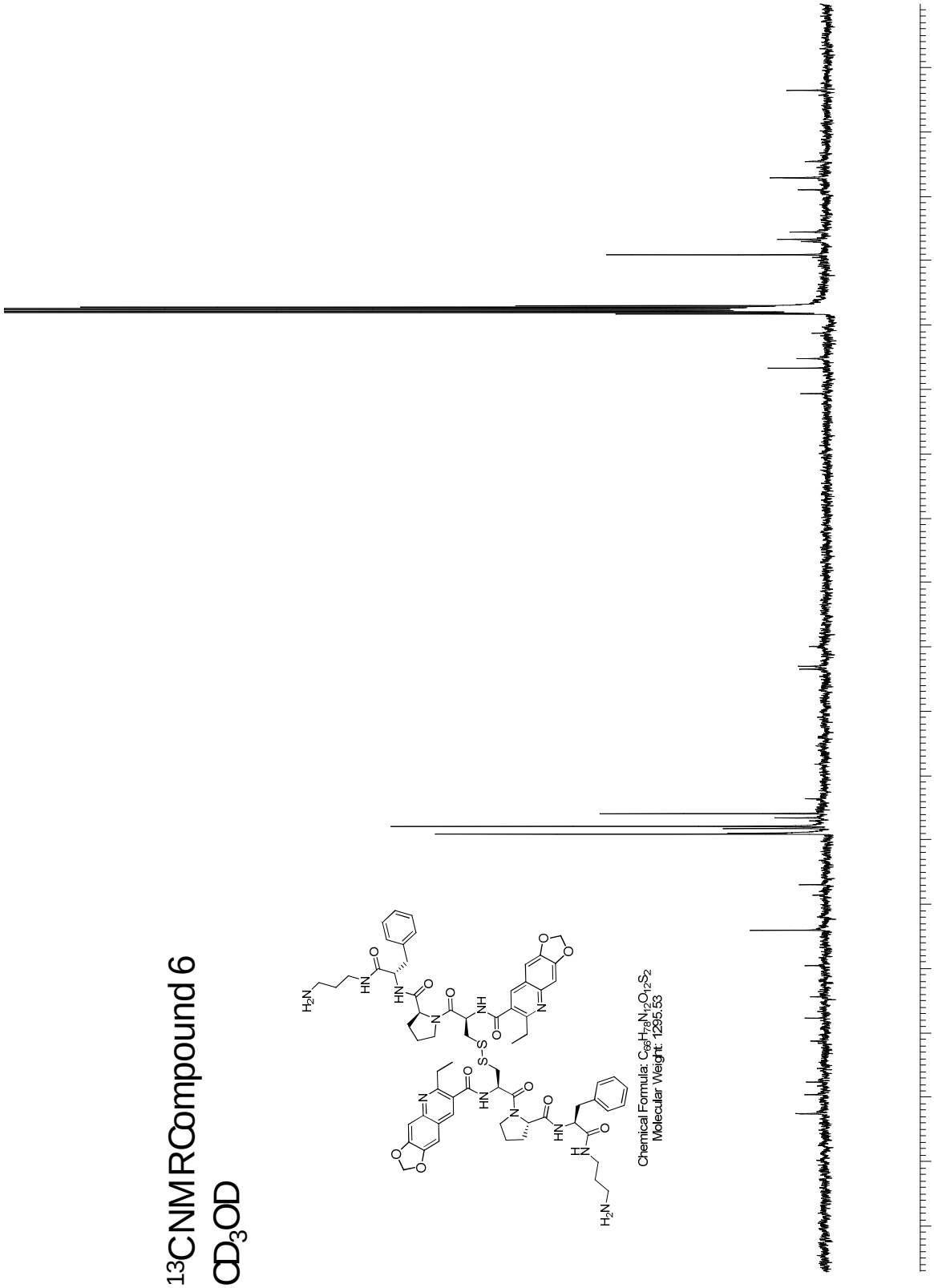
^{13}CNMR Compound 6
CD_3OD
Chemical Formula: $C_{68}H_{78}N_{12}O_{12}S_2$
Molecular Weight: 1295.53

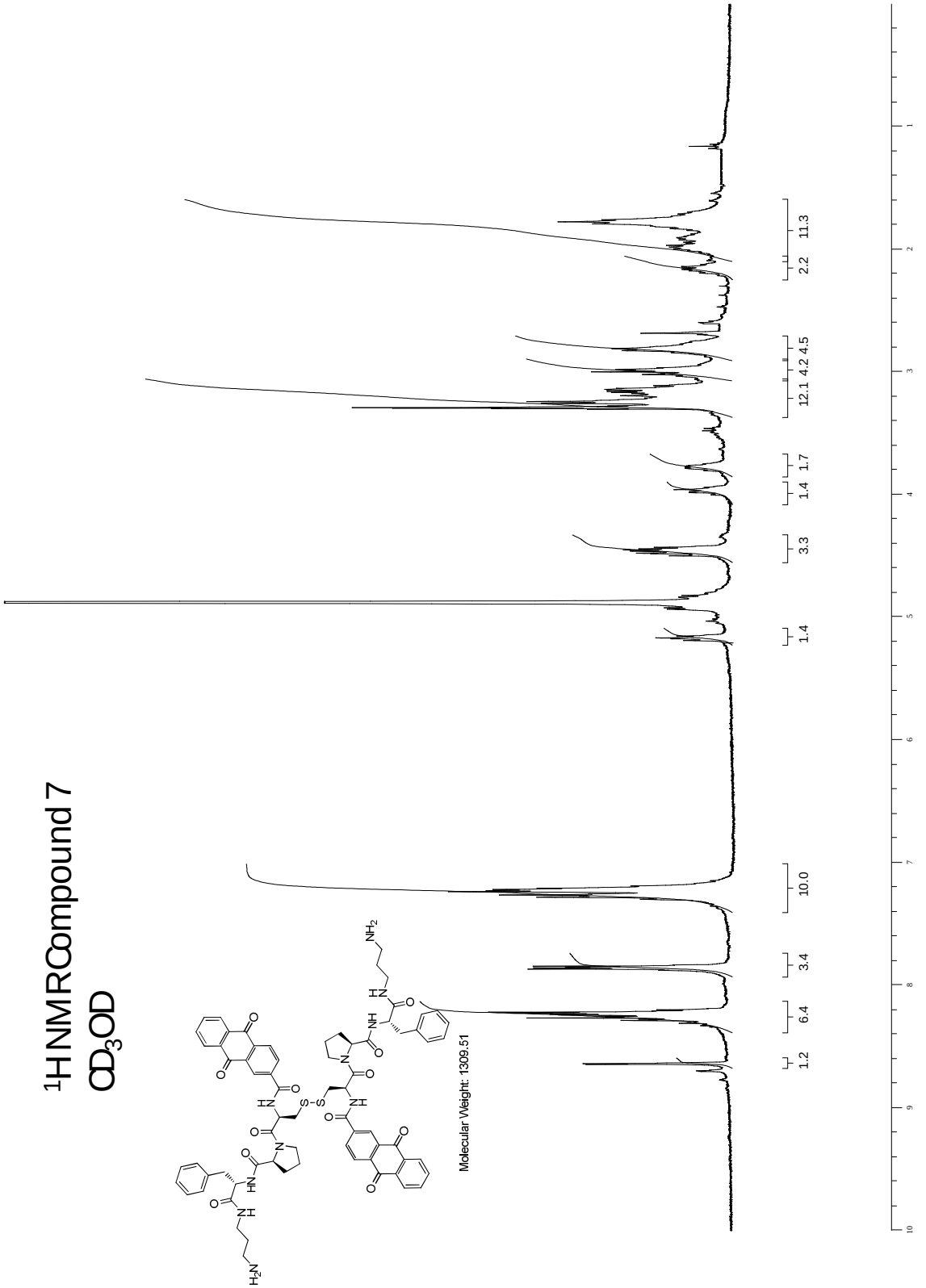
^{1}H NMR Compound 7
CD_3OD
Molecular Weight: 1309.51
1.2
6.4
3.4
10.0
1.4
3.3
1.4
1.7
12.1
4.2
4.5
2.2
11.3

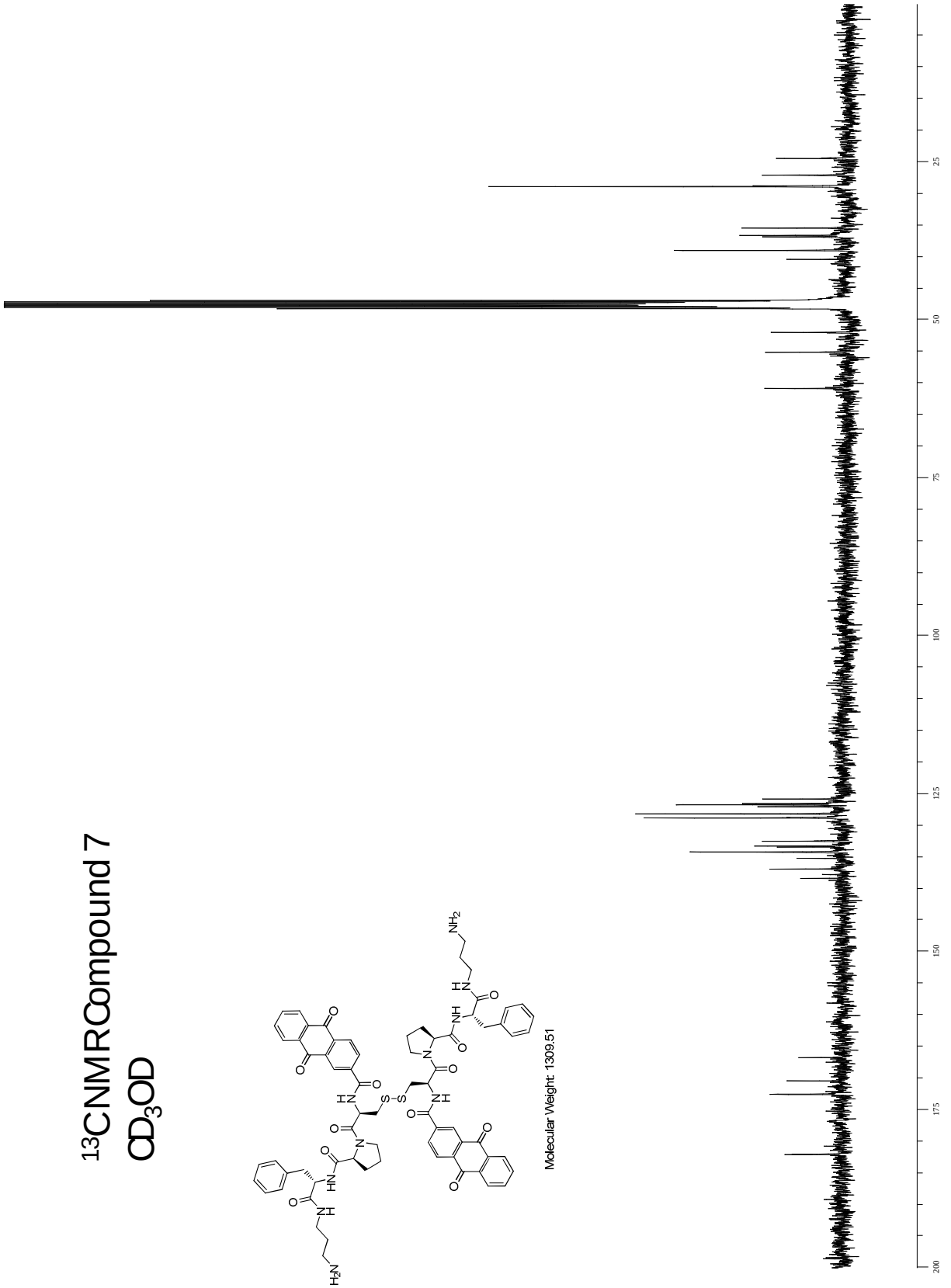
13CNMRCompound 7
CD3OD
Molecular Weight: 1309.51
25
50
75
100
125
150
175
200

Spectral data for compound 8

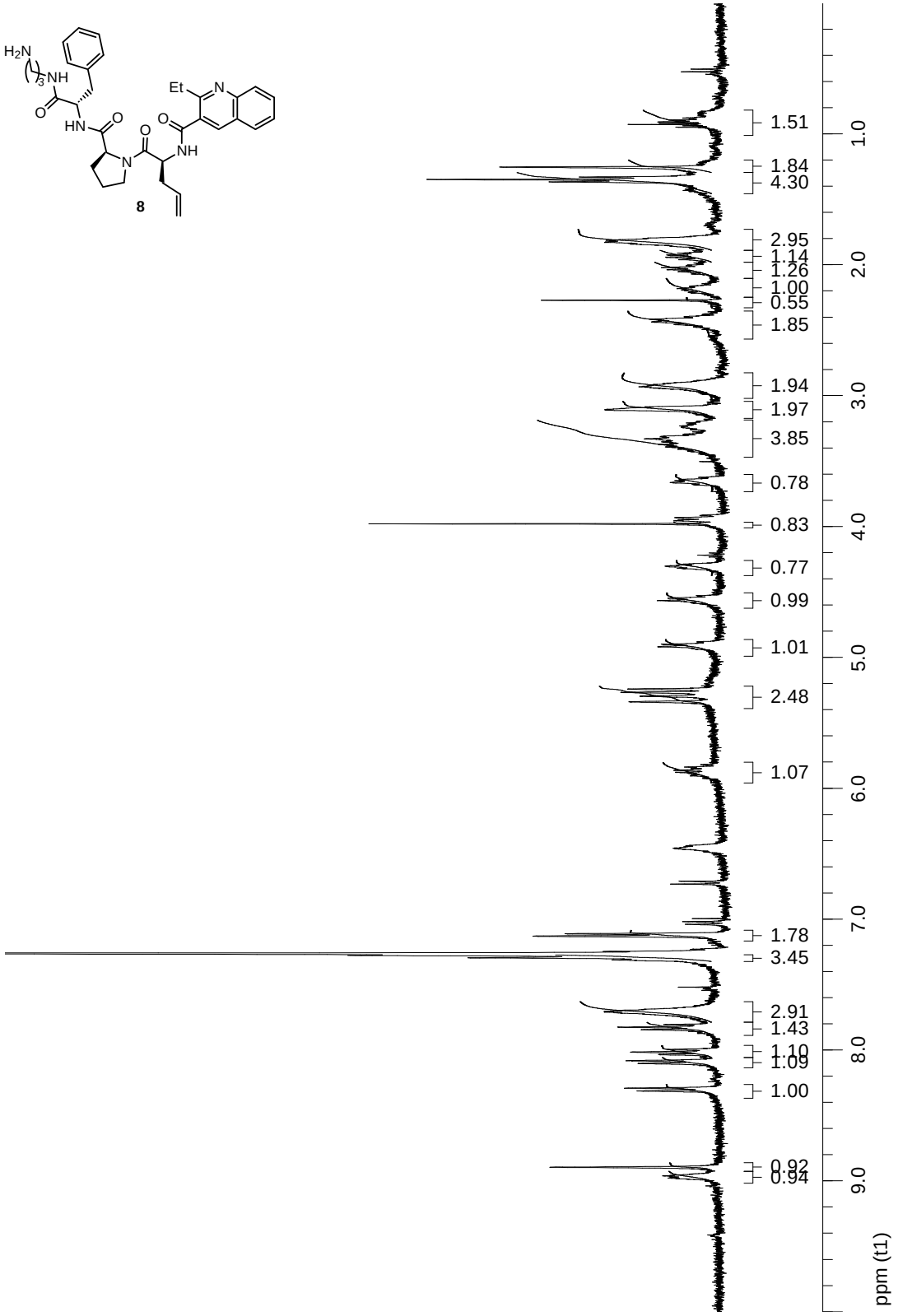

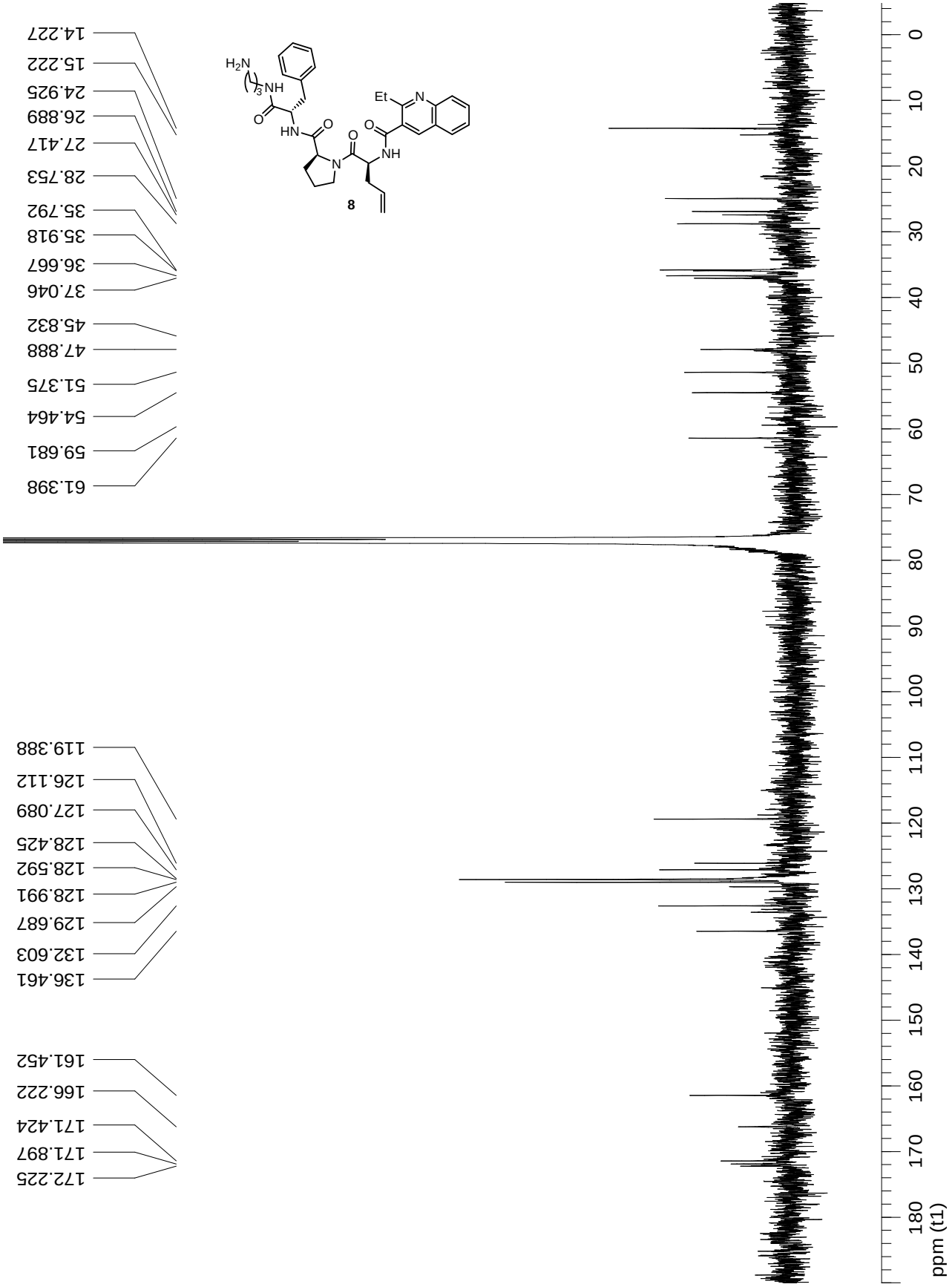
14.227
15.222
24.925
26.889
27.417
28.753
35.792
35.918
36.667
37.046
45.832
47.888
51.375
54.464
59.681
61.398
119.388
126.112
127.089
128.425
128.592
128.991
129.687
132.603
136.461
161.452
166.222
171.424
171.897
172.225
8
ppm (t1)

HPLC trace of the crude mixture of isomers **9 and 10:**

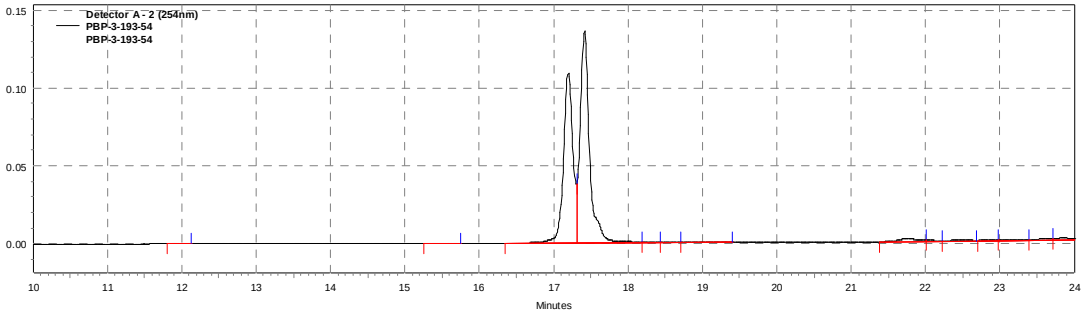

HPLC trace of pure **9:**

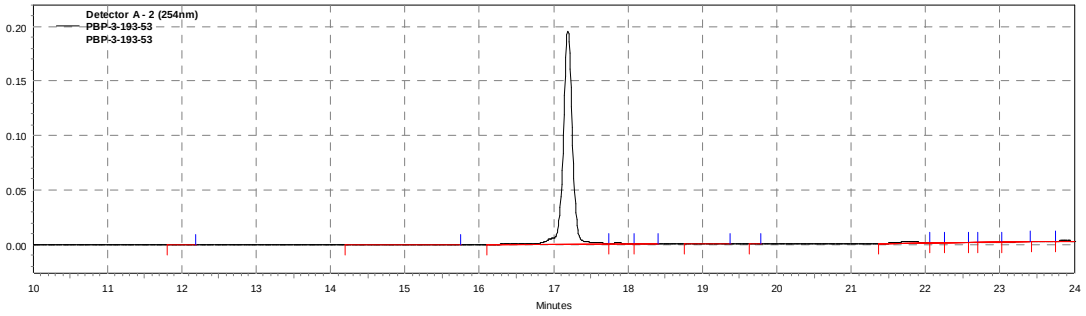

HPLC trace of pure **10:**

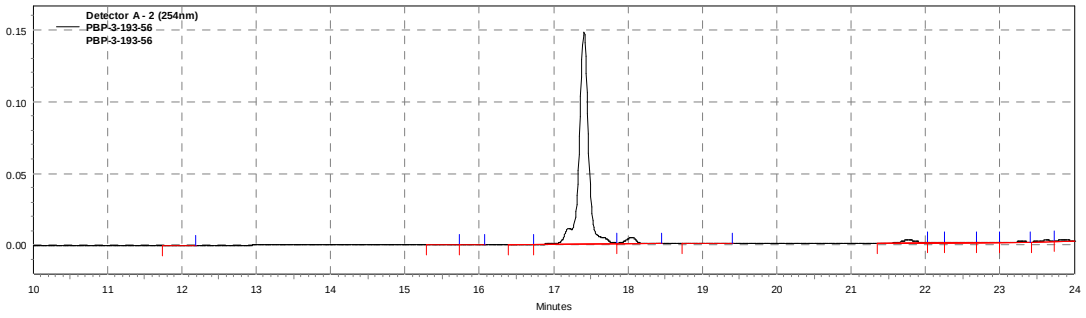

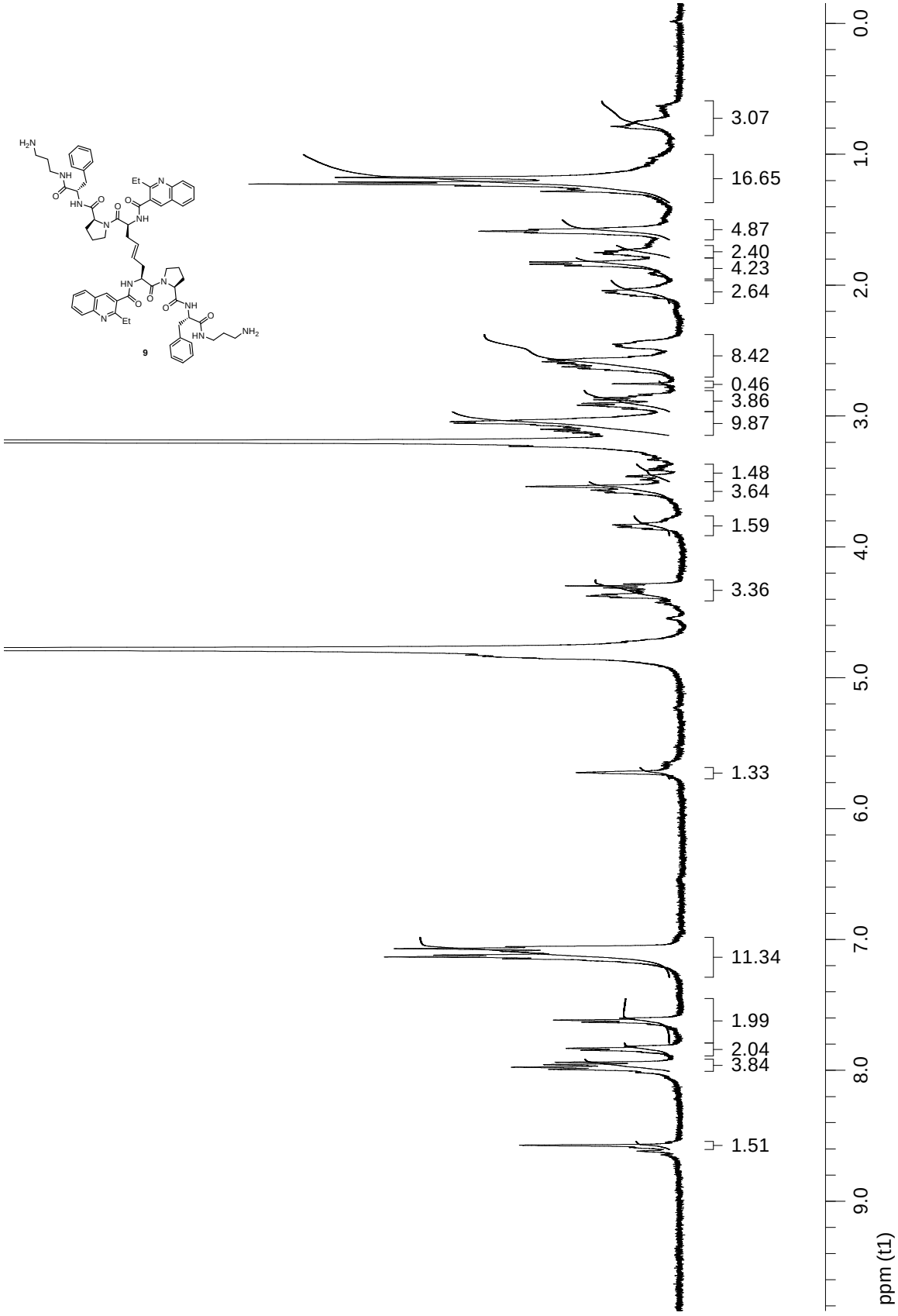
3.07
16.65
4.87
2.40
4.23
2.64
8.42
0.46
3.86
9.87
1.48
3.64
1.59
3.36
1.33
11.34
1.99
2.04
3.84
1.51
0.0
1.0
2.0
3.0
4.0
5.0
6.0
7.0
8.0
9.0
ppm (t1)

Compound **9**

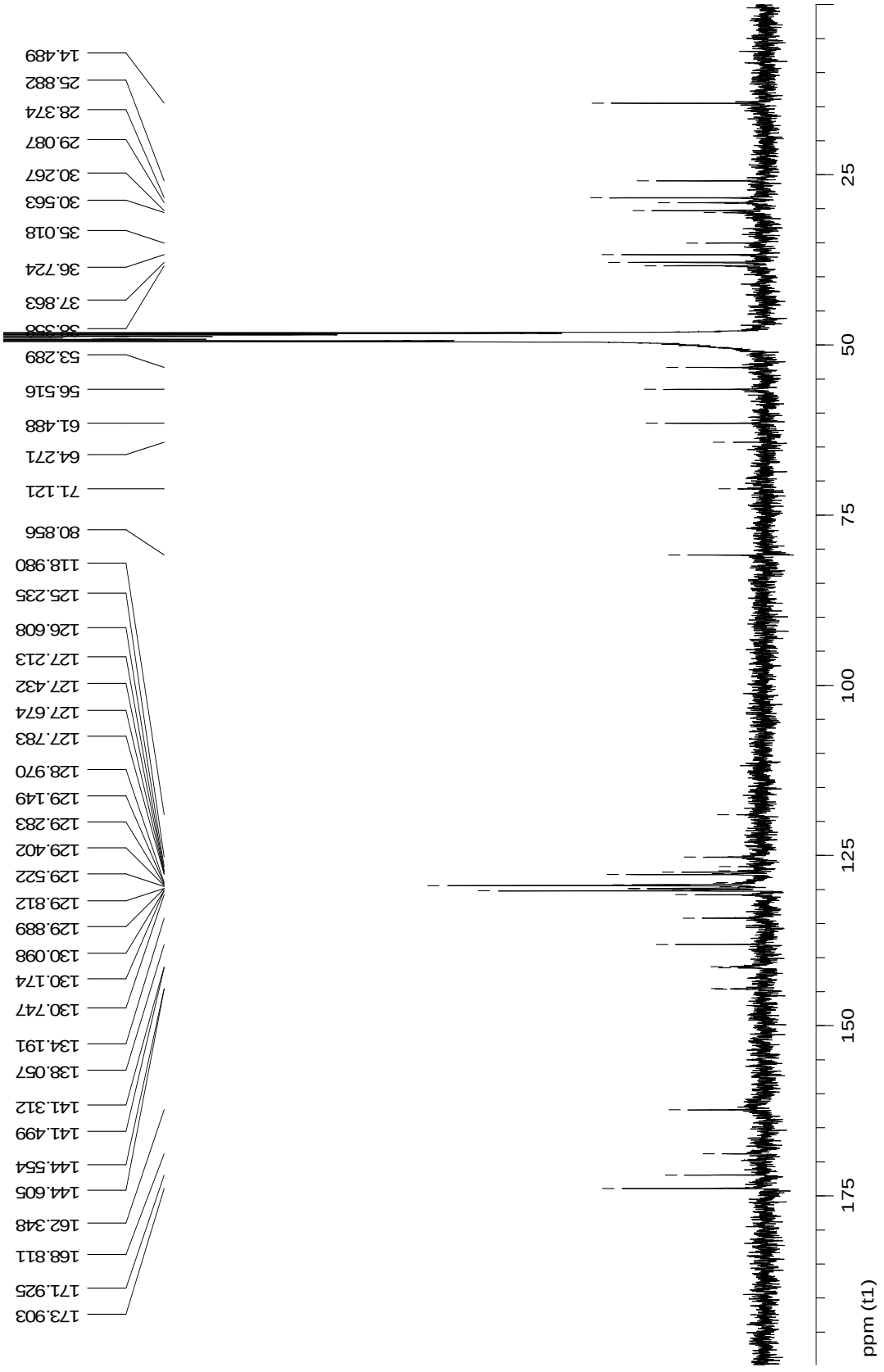
14.489
25.882
28.374
29.087
30.267
30.563
35.018
36.724
37.863
38.358
53.289
56.516
61.488
64.271
71.121
80.856
118.980
125.235
126.608
127.213
127.432
127.674
127.783
128.970
129.149
129.283
129.402
129.522
129.812
129.889
130.098
130.174
130.747
134.191
138.057
141.312
141.499
144.554
144.605
162.348
168.811
171.925
173.903
25
50
75
100
125
150
175
ppm (t1)

^{1}H-^{1}H COSY spectrum of 9 in CH_3OD

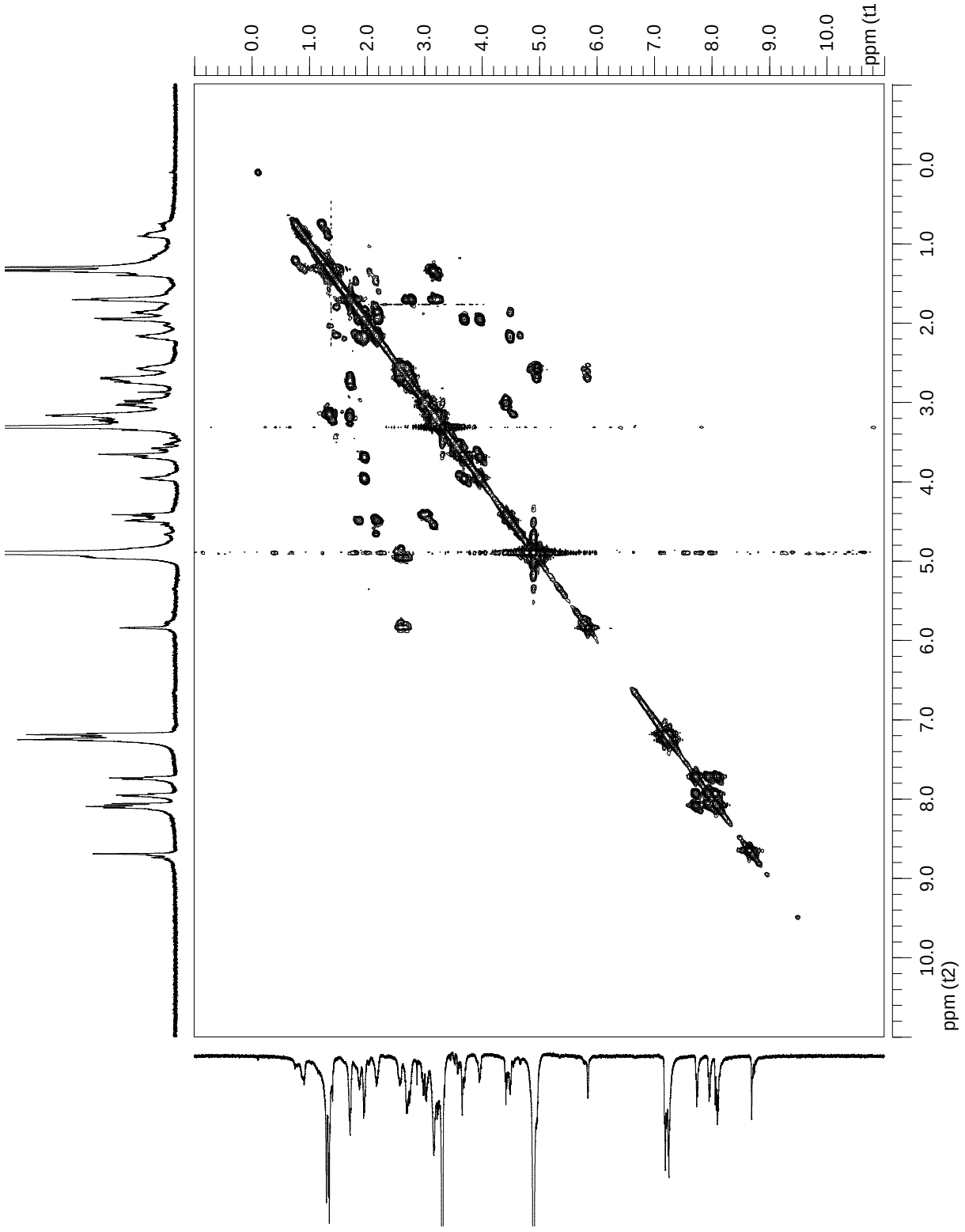

^{1}H-^{13}C HSQC spectrum of 9 in CH_3OD

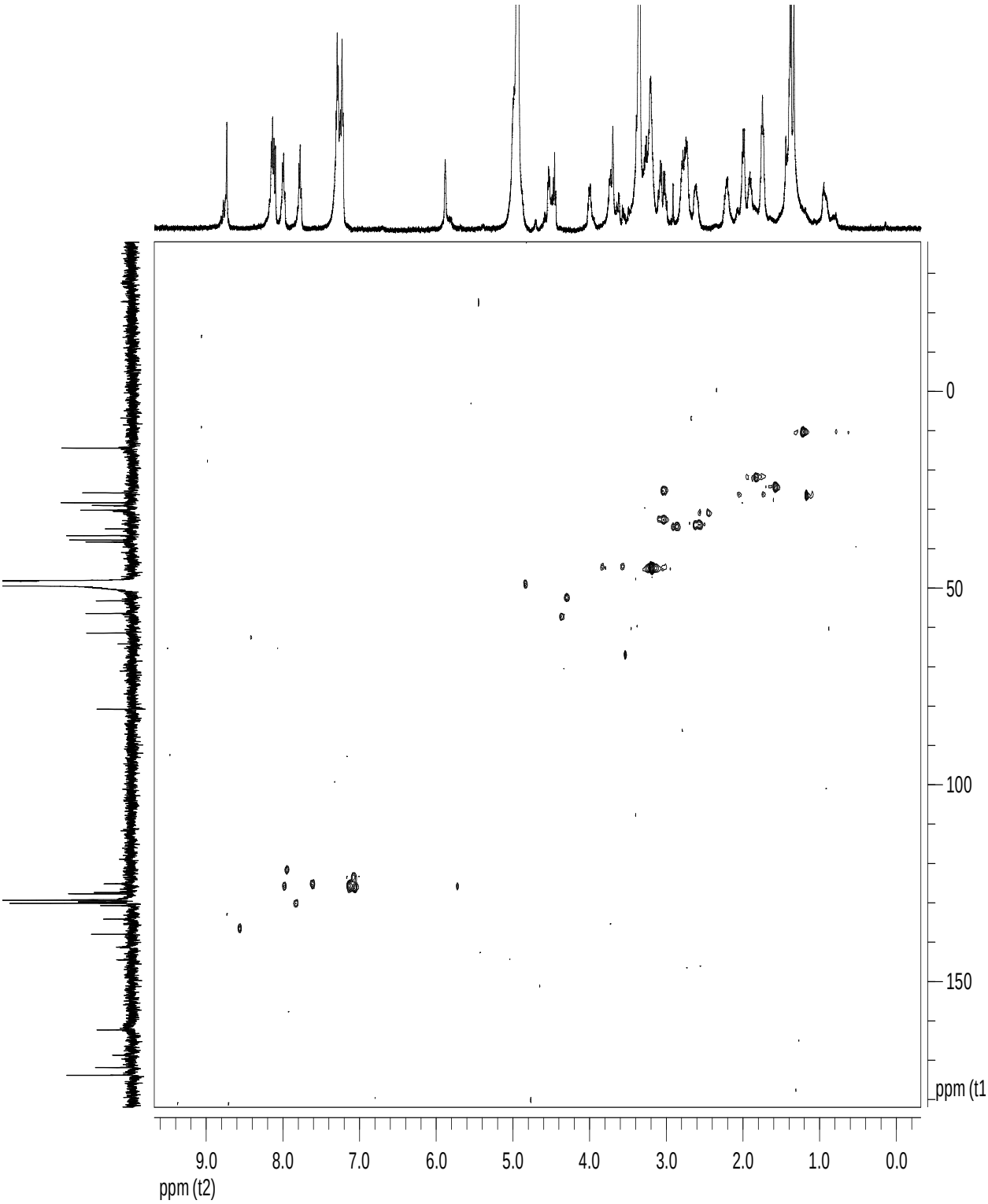

Spectral data for compound 10

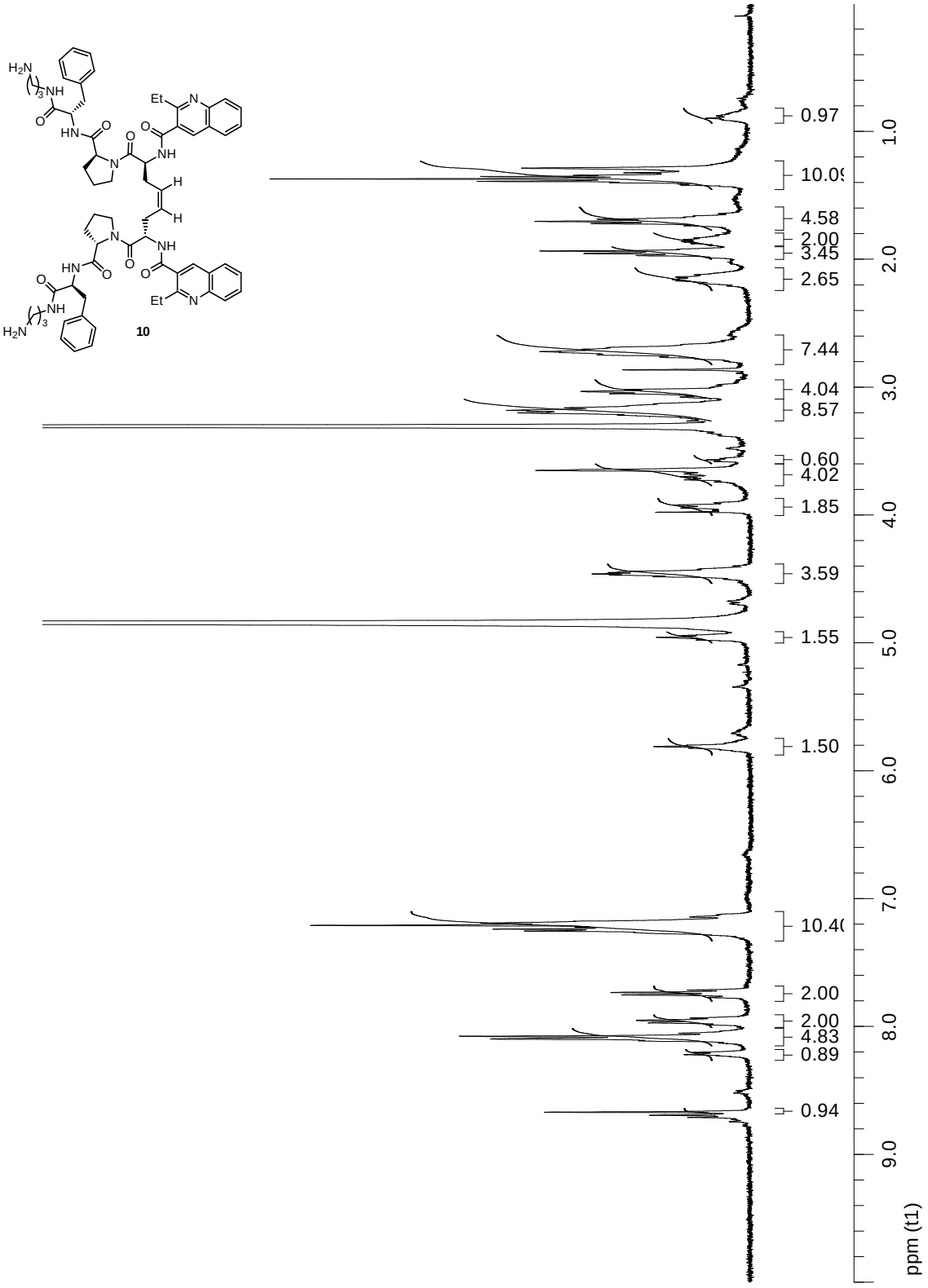

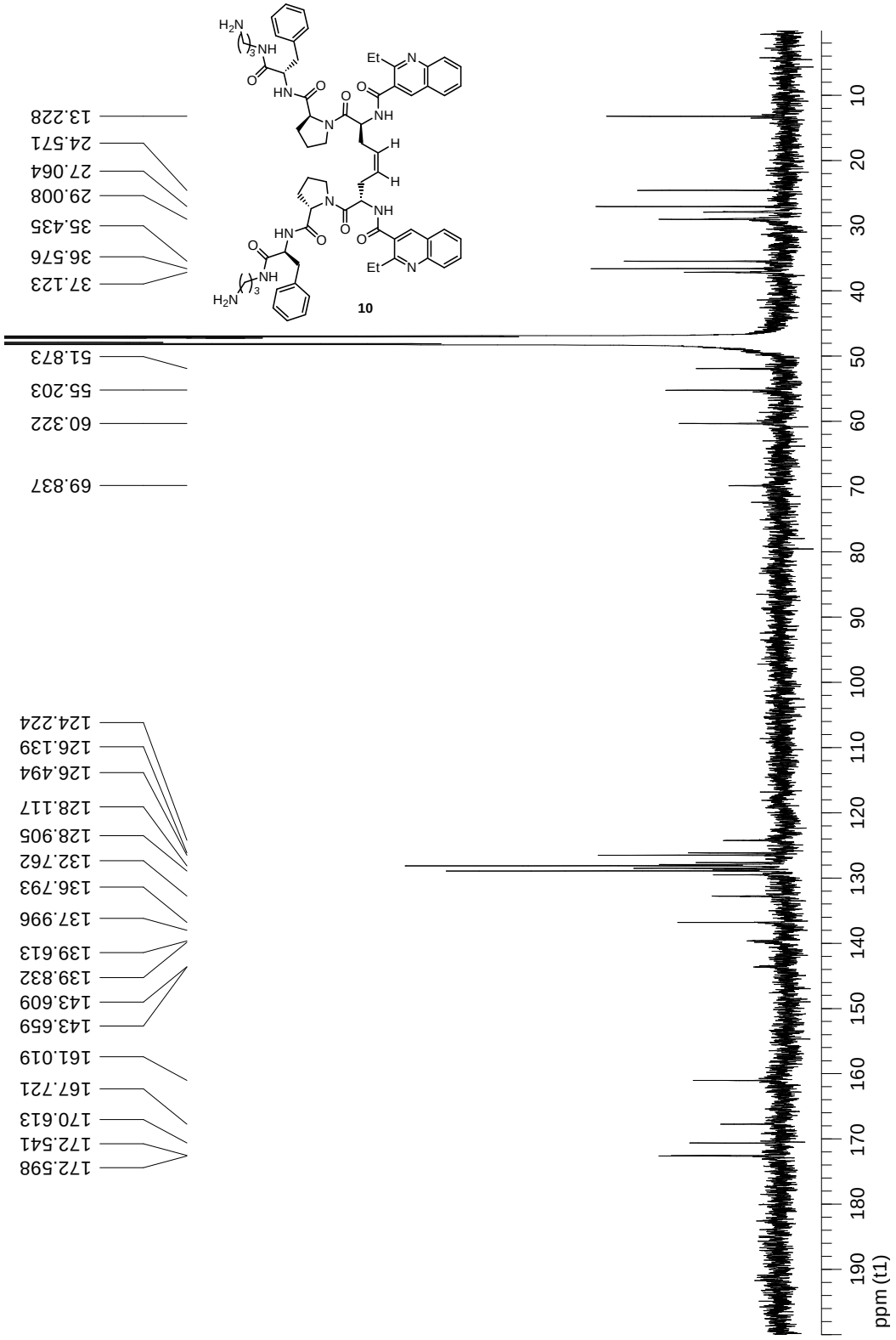
13.228
24.571
27.064
29.008
35.435
36.576
37.123
51.873
55.203
60.322
69.837
124.224
126.139
126.494
128.117
128.905
132.762
136.793
137.996
139.613
139.832
143.609
143.659
161.019
167.721
170.613
172.541
172.598
10
ppm (t1)

^{1}H-^{1}H COSY spectrum of 10 in CH_3OD

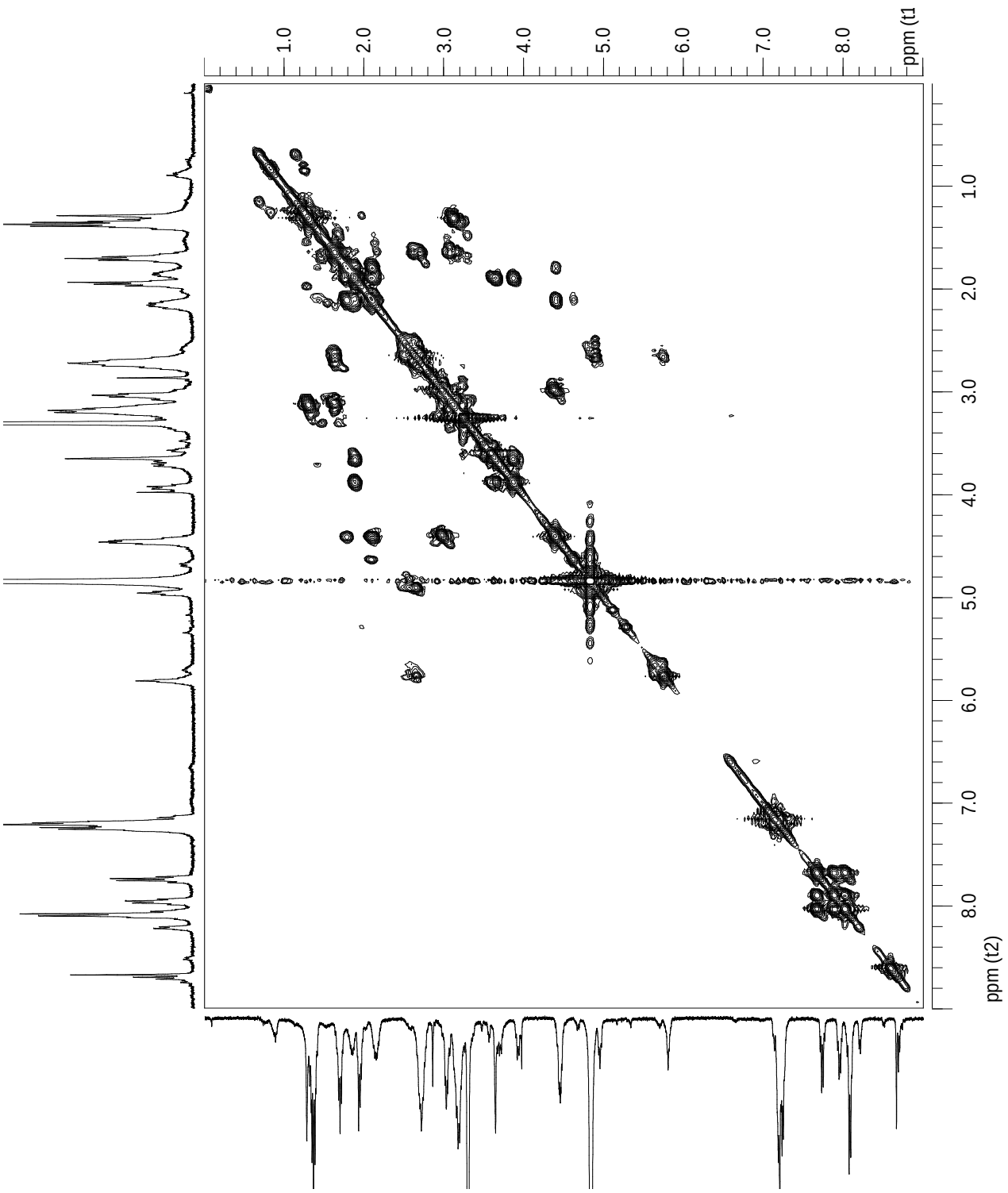

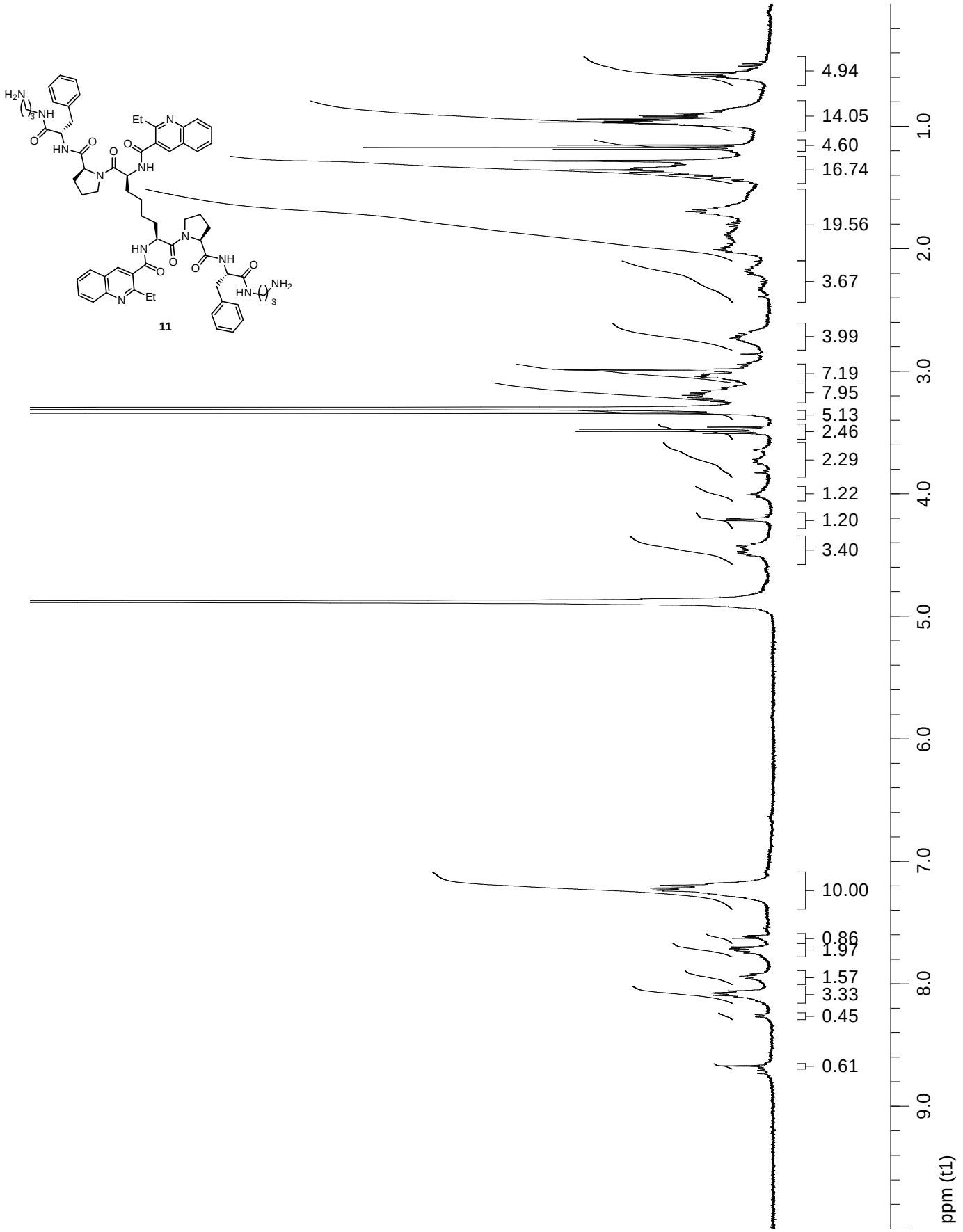
4.94
14.05
4.60
16.74
19.56
3.67
3.99
7.19
7.95
5.13
2.46
2.29
1.22
1.20
3.40
10.00
0.86
1.97
1.57
3.33
0.45
0.61
1.0
2.0
3.0
4.0
5.0
6.0
7.0
8.0
9.0
ppm (t1)

11

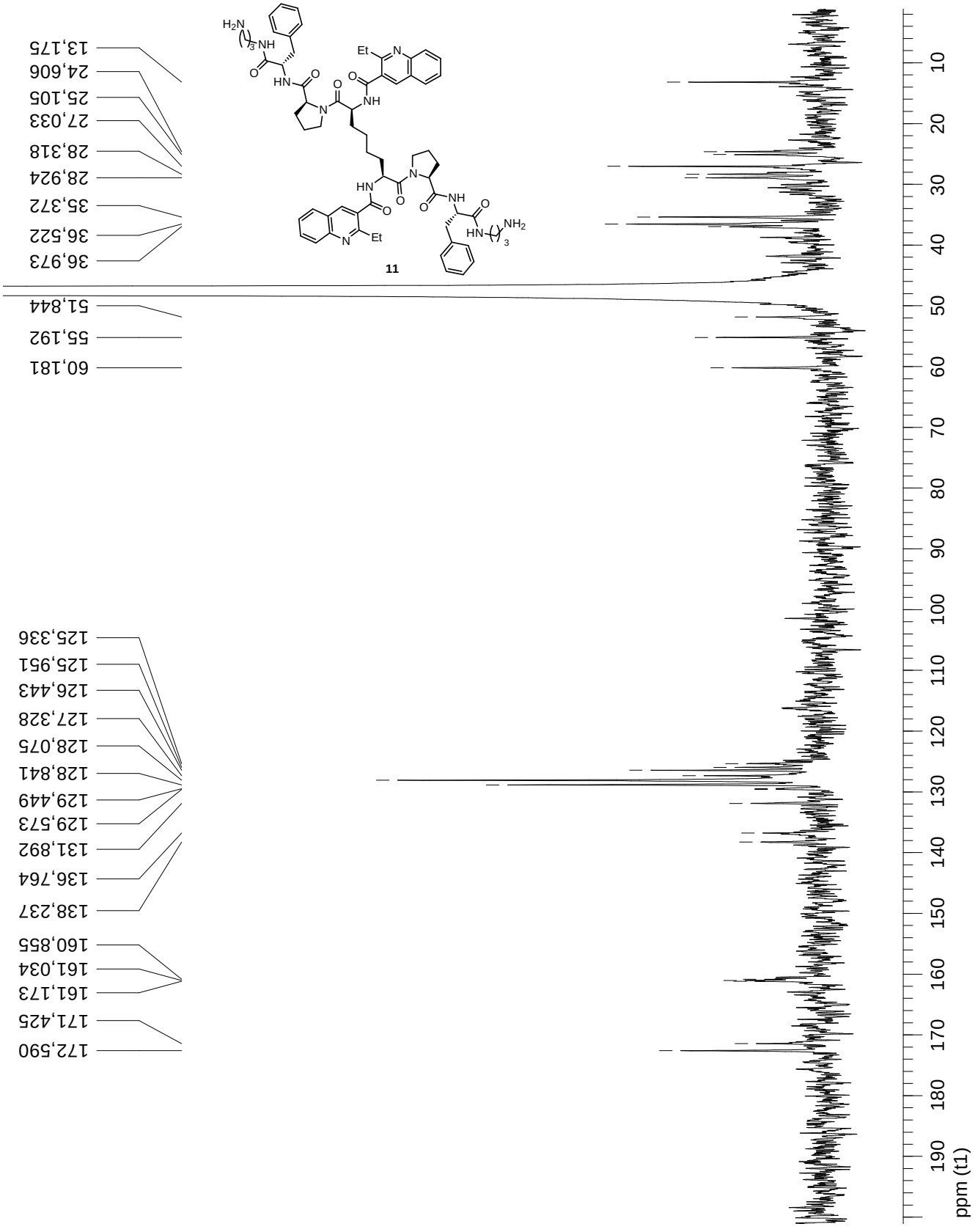
13,175
24,606
25,105
27,033
28,318
28,924
35,372
36,522
36,973
51,844
55,192
60,181
125,336
125,951
126,443
127,328
128,075
128,841
129,449
129,573
131,892
136,764
138,237
160,855
161,034
161,173
171,425
172,590
11
ppm (t1)

Assignment of *E* (9) and *Z* (10) Isomers

E and *Z* isomers were assigned by comparing the chemical shift value of their olefinic protons with those of (*E*)-4-octenedioic acid and (*Z*)-4-octenedioic acid, as previously reported by Kremminger, et al.[1] The analogy with these compounds suggests that the chemical shift value of the olefinic protons in the *E*-isomer should be downfield compared to those of the *Z*-isomer as shown in **Figure S1**. This assignment is also supported by the infrared spectra: ν C=C is at 1673.1 cm^{-1} for **9** (consistent with an *E* olefin), while this absorbance band is at 1664.3 cm^{-1} for **10** (consistent with a *Z* olefin).[2]

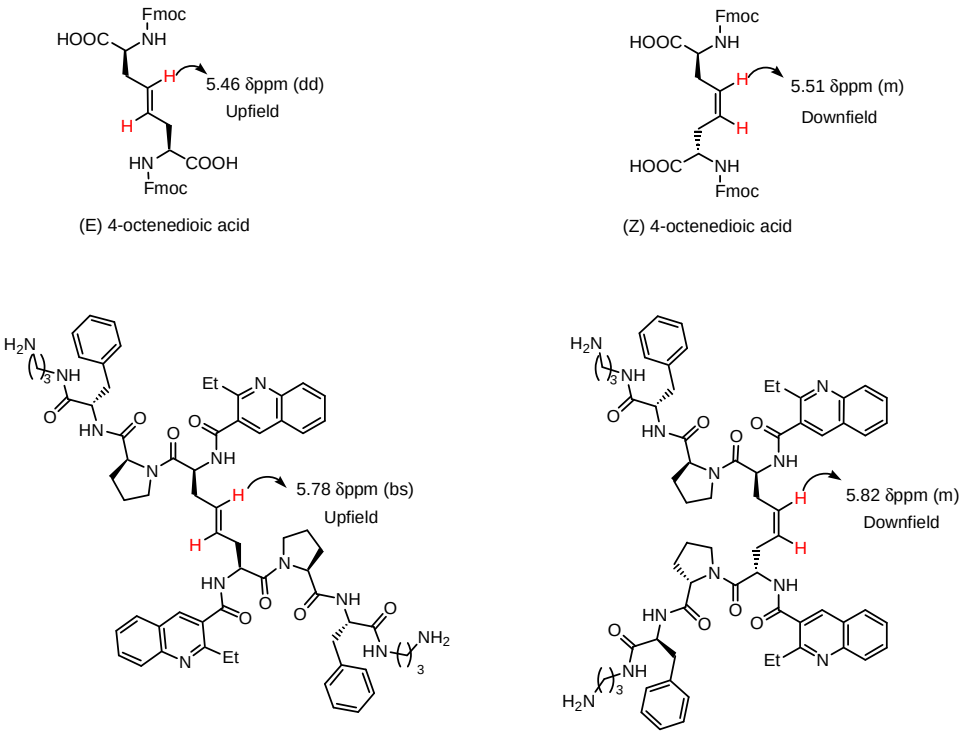

Figure S1. Assignment of *E* and *Z* isomers by analogy to *E* and *Z* 4-Octenedioc acid.

[1] Kremminger, P., Undheim, K. Asymmetric Synthesis of Unsaturated and Bis-Hydroxylated (S,S)-2,7-Diaminosuberic Acid Derivatives. *Tetrahedron* **1997**, 53, 6925-6936.

[2] Nakanishi, K. "Infrared Absorption Spectroscopy", Holden-Day, Inc., San Francisco, 1962, p. 24.

Binding Studies using fluorescence titrations:

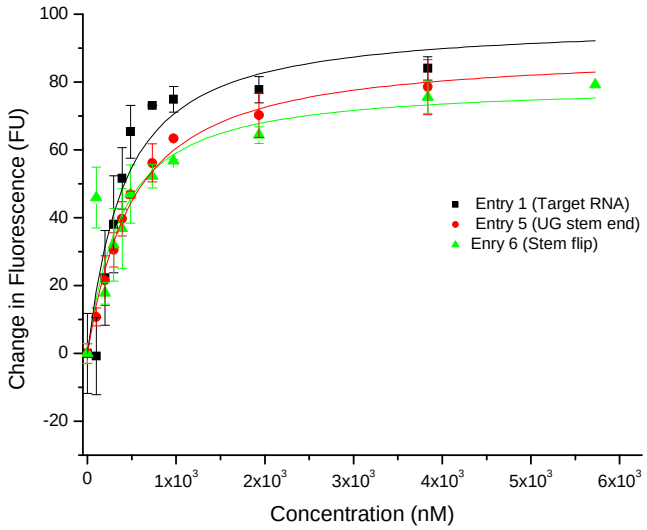

Figure S2: The effect of stem mutations on the binding affinity of **1.** Black: Sequence **1**. Red: Sequence **5**, Green: Sequence **6.** Each titration was performed in triplicate.

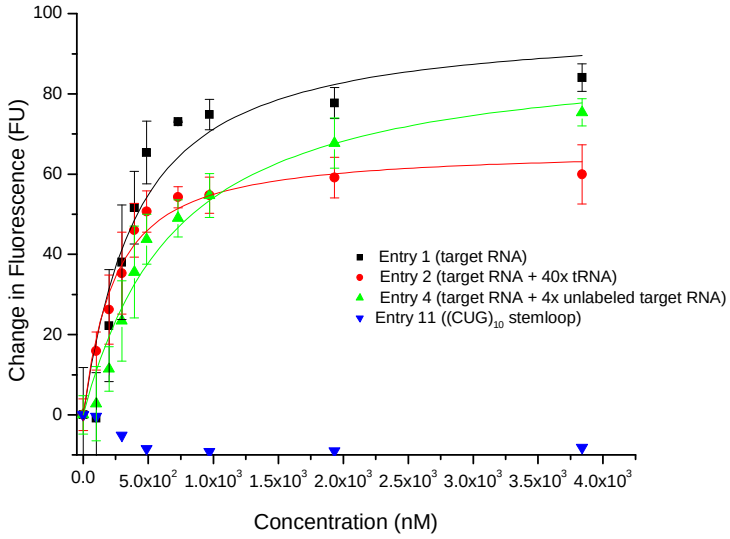

Figure S3: The effect of competition on the binding affinity of **1**. Black: Entry 1. Blue: Entry 11. Red: RNA Sequence 1 + 40 fold excess of mixed yeast tRNA (Entry 2). Green: RNA Sequence 1+ 4-fold excess Sequence 1 (unlabeled target) (Entry 4). Each titration was performed in triplicate.

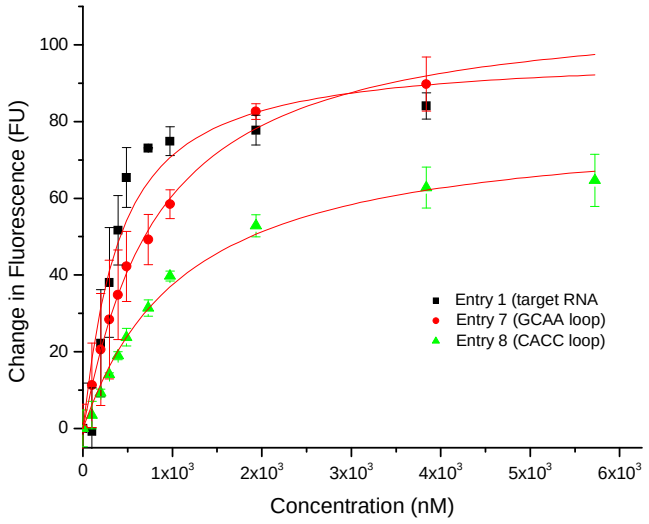

Figure S4: The effect of loop mutations on the binding affinity of **1**. Black: Entry 1 Red: Entry 7, Green: Entry 8. Each titration was performed in triplicate.

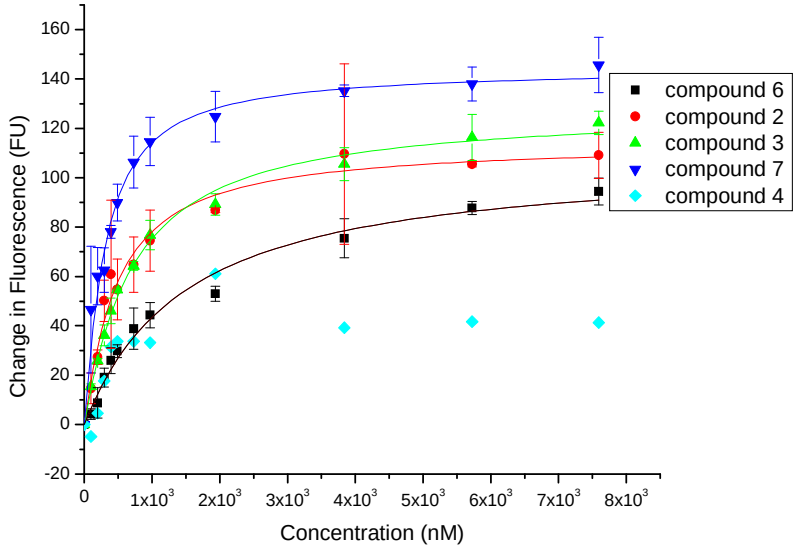

Figure S5. Fluorescence titrations for compounds **2, 3, 4, 5, 6,** and **7** and RNA sequence 1. Each experiment was repeated at least 2 times

The fluorescence titration for compound **5** is shown along with filter-binding assays on page S31.

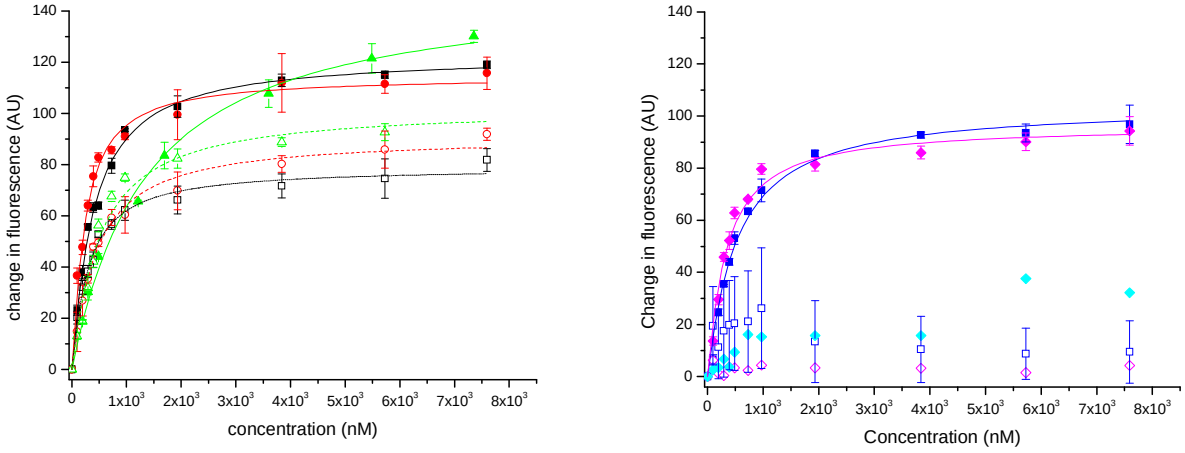

Figure S6. Binding isotherms obtained by plotting the change in dilution corrected fluorescence of Cy-3 labeled FSS RNA as a function of the ligand concentration. Data were fit to a one-site binding model accounting for ligand depletion as described in the main text. Left: **9** (■), **10** (●), and **11** (▲) in the absence (closed symbols) or presence (open symbols) of competitor tRNA; Right: **8** (■), 2-ethylquinoline 3-carboxylic acid (♦), and **5** (♦) in the absence (closed symbols) or presence (open symbols) of competitor tRNA. As compound **5** did not display any affinity for the target FSS alone, it was not examined in the presence of competitor tRNA.

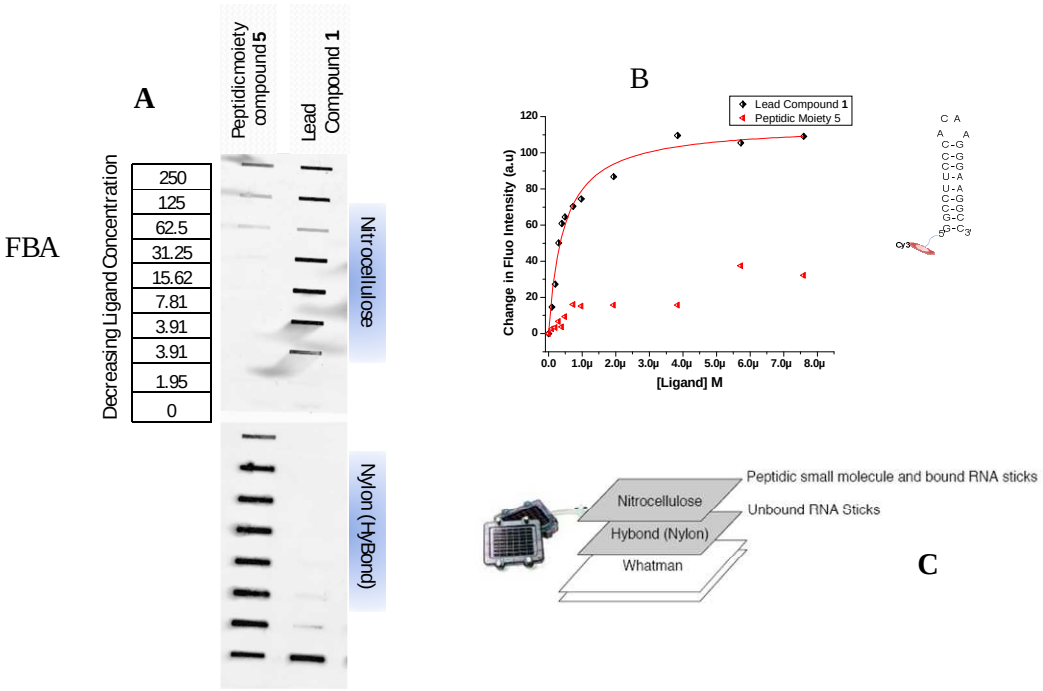

Figure S7 (A) Filter binding assay (FBA) of compound **5** relative to lead compound **1**. (B) Binding isotherm for fluorescence titration of compound **5** and **1.** Both assays confirm the poor binding affinity of **5** towards the FSS RNA (C) schematic of the FBA assay used**.**

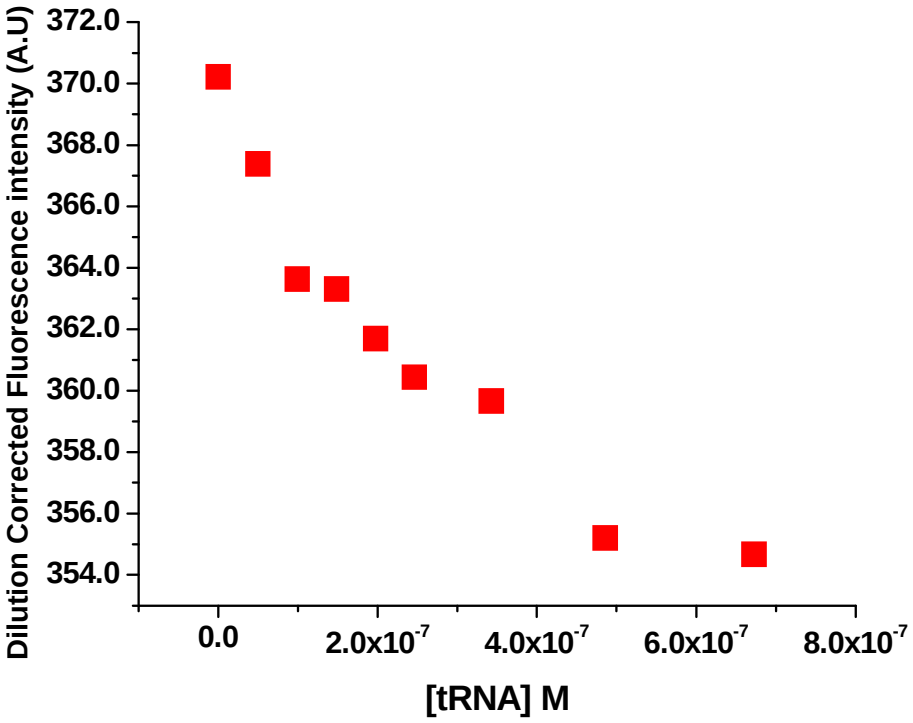

Titration of yeast tRNA into Cy3-labeled RNA sequence 1. Fluorescence intensity was measured at 564 nm as in experiments detailed above.

Protocol for Binding Studies Using SPR

Materials: Interaction analyses were performed using a Biacore®-X (Biacore AB, Uppsala, Sweden) optical biosensor equipped with research-grade CM5 sensor chips (GE Healthcare, Piscataway, NJ, USA). Amine-coupling reagents (N-ethyl-N′-(3-dimethylaminopropyl)carbodiimide [EDC], N-hydroxysuccinimide [NHS], and ethanolamine HCl) were purchased from Sigma Aldrich (St. Louis, MO, USA). Streptavidin was purchased from Rockland (Gilbertsville, PA, USA) and the biotinylated HIV-1 FSS RNA was purchased from Integrated DNA Technologies, Inc. (Coralville, IA, USA)

Step I: Instrument preparation

The Biacore® X instrument was cleaned using a "desorb" method at 25 °C to remove any proteins adsorbed to the IFC channels. After docking a maintenance chip, the instrument was primed with desorb solution 1 (0.5% sodium dodecyl sulfate [SDS]), followed by water, desorb solution 2 (50 mM glycine, pH 9.5), and finally, three times with water. The working area around the instrument was pretreated with RNase*Zap* (Ambion, Austin, TX, USA) to inactivate any ribonucleases.

Step II: Running buffer preparation

Autoclaved 1X Phosphate-Buffered Saline (PBS) (4.3 mM Na_2HPO_4, 1.47 mM KH_2PO_4, 137 mM NaCl, 2.7 mM KCl) with 5 mM $MgCl_2$ and 0.005 % Tween 20 (pH = 7.24) was used as a running buffer. The buffer was filtered to remove any particulate matter and degassed using house vacuum to minimize air spikes in the response data.

Step III: Sensor chip preconditioning

The CM5 sensor chip and the running buffer were equilibrated to room temperature before use. After docking the chip and priming the instrument three times with the running buffer, dextran layer coating the chip surface was cleaned and hydrated with three consecutive 100 μL injections each of 100 mM HCl and 50 mM NaOH at a flow rate of 100 μL/min, flowing them over both the flow cells.

Step IV: Streptavidin Immobilization

Streptavidin was immobilized on both the flow cells of the preconditioned CM5 sensor chip surface using standard amine-coupling chemistry. The surface of the flow cells was activated at 25 °C with a 35 μL injection of a 1:1 mixture of 0.4 M EDC and 0.1 M NHS at a flow rate of 5 μL/min. To create a high-density surface, 35 μL of 250 μg/mL solution of streptavidin in 10 mM sodium acetate (pH 5.0) was injected at a flow rate of 5 μL/min. The same injection was repeated over flow cell 2 only for immobilizing equivalent amount of streptavidin on both the flow cells. Finally, 35 μL of 1.0 M ethanolamine (pH 8.5) was injected across the flow cells for 7 min (flow rate = 5 μL/min) to deactivate the surfaces. To remove any electrostatically bound streptavidin from the flow cells, 15 μL of 0.1 M HPO_4 was injected at a

flow rate of 5 μL/min. Using this procedure, approximately 5500 RU of streptavidin was immobilized on each flow cell.

Step V: Biotinylated HIV-1 FSS RNA immobilization

Flow cell 2 was assigned as a reference cell to subtract nonspecific binding, drift, and bulk refractive index. A solution of 50 μM biotinylated HIV-1 FSS RNA in running buffer was heated to 65 °C for 4 min and allowed to cool slowly to RT (in the presence of 5 mM $MgCl_2$ present in the running buffer) in order to ensure that the RNA assumes its secondary stem-loop structure. For immobilization of the RNA, two consecutive 35 μL injections of 50 μM biotinylated HIV-1 FSS RNA in running buffer were injected over flow cell 1 for 7 min each (flow rate = 5 μL/min). Using this procedure, approximately 870 RU of the HIV-1 FSS RNA was immobilized on to the sensor chip. Finally, 35 μL of Biotin (200 μg/mL) was injected over both the flow cells at a flow rate of 5 μL/min to block remaining biotin binding sites on the streptavidin. Similarly, two other surface density chips (460 RU and 1160 RU) were prepared by varying the concentration of HIV-1 FSS RNA injected on the flow cell 2.

Step VI: Compound dilutions

A 5 mM stock solution of compounds to be analyzed for their binding affinity to HIV-1 FSS RNA was prepared in degassed deionized water. Further dilutions were then made in the running buffer (to avoid bulk drifts caused by the change in the refractive index) to produce concentrations of 250, 100, 50, 40, 30, 20, 10, 5, 1 and 0.5 μM

Step VII: Binding analysis

All binding experiments were done at 25 °C and at a flow rate of 80 μL/ min. Data collection rate was set at 2.5 Hz. The instrument with the HIV-1 FSS RNA immobilized chip was primed three times with the running buffer. Prior to the analysis, 80 μL of the running buffer (buffer blank) was injected to ensure that the instrument was fully equilibrated. Response data were then collected for the compounds binding to the HIV-1 FSS RNA immobilized surfaces. For each series of compound dilutions, 80 μL injections were made for 1 min, going from the lowest to the highest concentration. The dissociation phase was monitored for 100 seconds followed by a wash cycle (no regeneration reagent was used). After every three injections of the compound, one buffer injection was made for double referencing.

Step VIII: Kinetic analysis

Data processing and kinetic analysis were performed using BIAevaluation software (version 4, Uppsala, Sweden). Relative response units were obtained by zeroing the y-axis at approximately 10-15 s before the start of the association phase. The start times of all injections were aligned, and the binding responses were corrected for the signals from the reference surface and from buffer blanks (to removes systematic drifts). Processed data were globally fit to a simple 1:1 (Langmuir) binding model.

SPR data for compound 1:

For compound **1** the kinetic parameters were measured on two different density surfaces (**Figure S8** and **Figure S9**). Kinetic parameters calculated from different surfaces with different flow rates are in high conformity with each other as shown in **Table S1.**

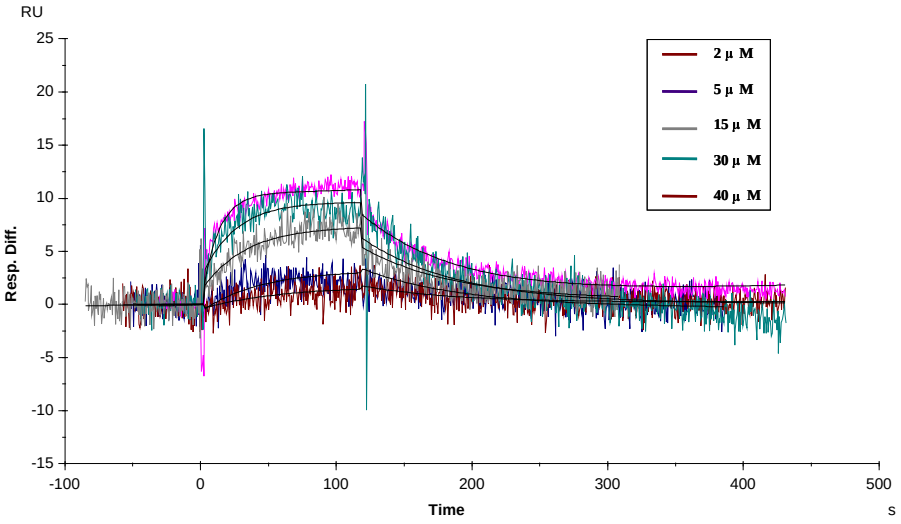

Figure S8. Sensorgrams to evaluate the binding kinetics for interaction of **1** with the HIV-1 FSS RNA at 25 °C. Data was collected on a chip with approximately 460 RU HIV-1 FSS RNA immobilized on its surface. Different concentrations (as indicated in the insert) of **1** (80 µL) were injected at a flow rate of 40 µL/min at 25 °C. The association phase continued for 2 minutes after which the dissociation phase was observed for 5.5 minutes. The sensorgarms were fit globally to 1:1 binding model using BIAevaluation software.

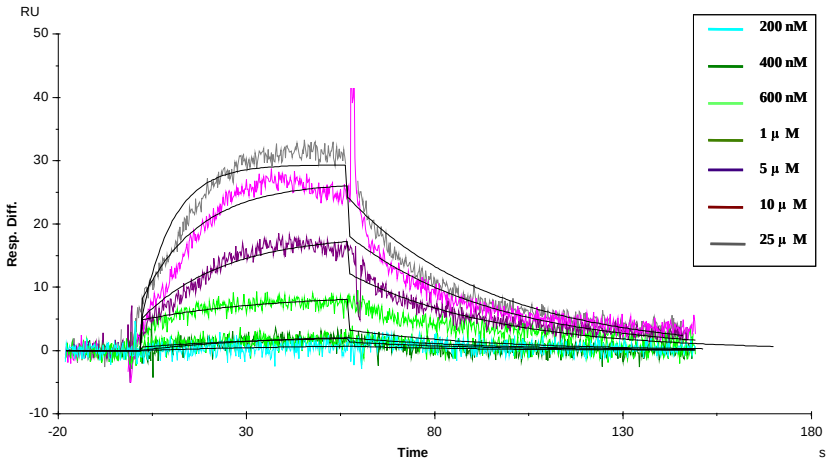

Figure S9 Sensorgrams to evaluate the binding kinetics for interaction of **1** with the HIV-1 FSS RNA at 25 °C. Data was collected on a chip with approximately 1160 RU HIV-1 FSS RNA immobilized on its surface. Different concentrations (as indicated in the insert) of 4.1-4.1 (80 µL) were injected at a flow rate of 80 µL/min at 25 °C. The association phase continued for 1 minute after which the dissociation phase was

observed for 1.5 minutes. The sensorgarms were fit globally to 1:1 binding model using BIAevaluation software.

Table S1. Kinetic data for interaction of **1** measured at different surface densities (HIV-1 FSS RNA immobilization) and different flow rates. Both data sets were collected at 25 °C.

Ligand	Surface Density (RU)	Flow Rate (µL/min)	Dissociation rate (k_{off}) s^{-1}	Association rate (k_{on}) $M^{-1}s^{-1}$	Dissociation Constant (K_D) µM	Chi^2
1	460	40	1.41×10^{-2}	1.79×10^{3}	7.88	1.07
1	1160	80	1.08×10^{-2}	1.48×10^{3}	7.30	2.06

SPR data for compounds 9 and 10:

Binding kinetics for **9** and **10** were measured on a low density (460 RU) surface as shown in **Figure S10** and **Figure S11**.

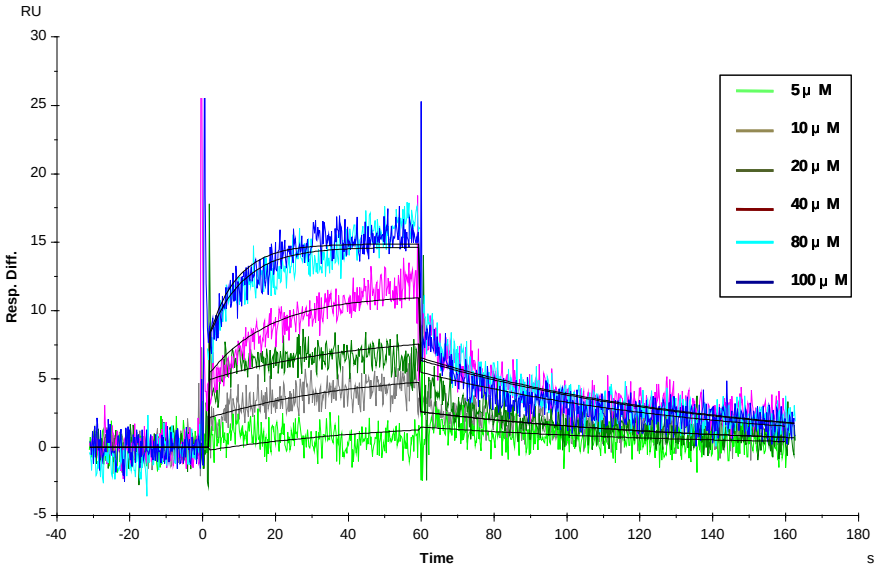

Figure S10. Sensorgrams to evaluate the binding kinetics for interaction of compound **9** with the HIV-1 FSS RNA at 25 °C. Data was collected on a chip with approximately 460 RU HIV-1 FSS RNA immobilized on its surface. Different concentrations (as indicated in the insert) of compound **9** (80 µL) were injected at a flow rate of 80 µL/min at 25 °C. The association phase continued for 1 minute after which the dissociation phase was observed for approximately 2 minutes. The sensorgarms were fit globally to a 1:1 binding model using BIAevaluation software.

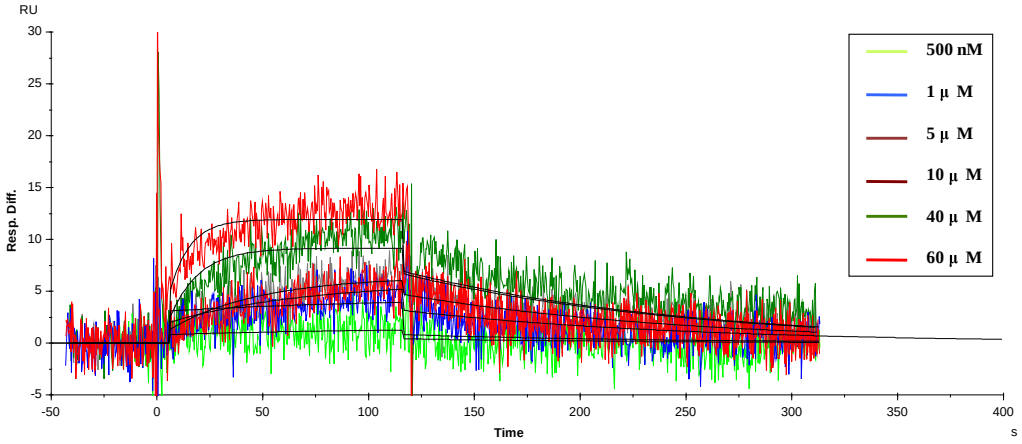

Figure S11. Sensorgrams to evaluate the binding kinetics for interaction of compound **10** with the HIV-1 FSS RNA at 25 °C. Data was collected on a chip with approximately 460 RU HIV-1 FSS RNA immobilized on its surface. Different concentrations (as indicated in the insert) compound **10** (80 µL) were injected at a flow rate of 40 µL/min at 25 °C. The association phase continued for 2 minutes after which the dissociation phase was observed for approximately 3 minutes. The sensorgarms were fit globally to 1:1 binding model using BIAevaluation software.

SPR data for compound 11:

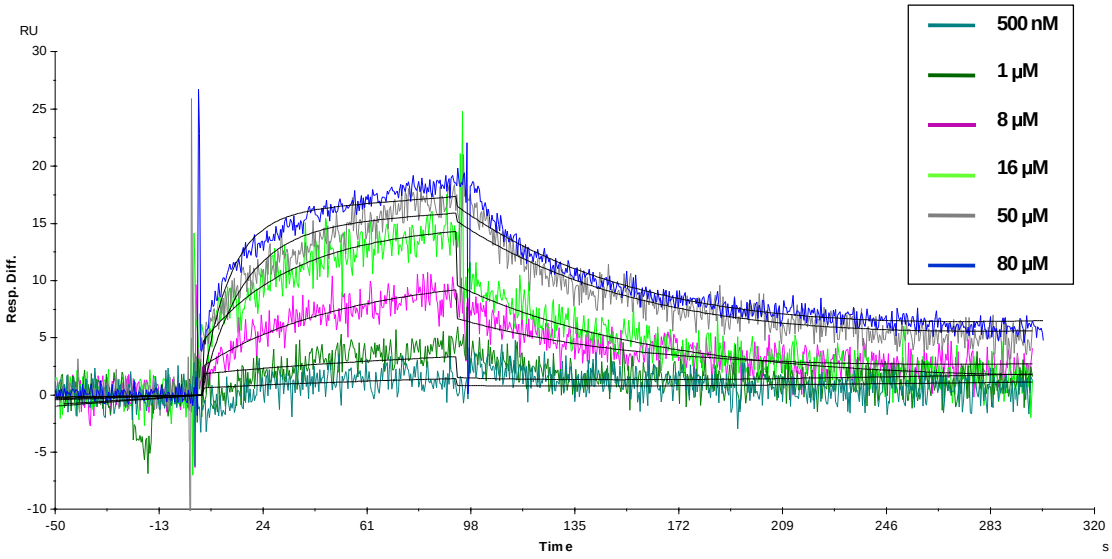

Figure S12. Representative data obtained from the SPR experiments showing association and dissociation phases of interaction between **11** and the biotinylated HIV-1 FSS RNA (870 RU) immobilized on the sensor surface. Various concentrations of **11** were injected (80 µL) in the running buffer at a flow rate of 50 µL/min. The dissociation phase was monitored for 200 seconds. Two buffer injections, 80 µL each were used for regeneration of the surface after dissociation phase. Data were fit globally fit to a simple 1:1 (Langmuir) binding model with baseline drift.

Comparison with Neomycin: Binding of neomycin sulfate was analyzed using similar experimental procedures as those shown above. Data was collected on a chip with approximately 255 RU HIV-1 FSS RNA immobilized on its surface. Different concentrations (as indicated in the insert) of neomycin were injected at a flow rate of 60 µL/min at 25 °C. Sensorgrams show insufficient curvature to derive reliable kinetic constants, but appear to show very fast on and off rates. The dissociation constant was determined via steady-state analysis to be 2.6 µM.

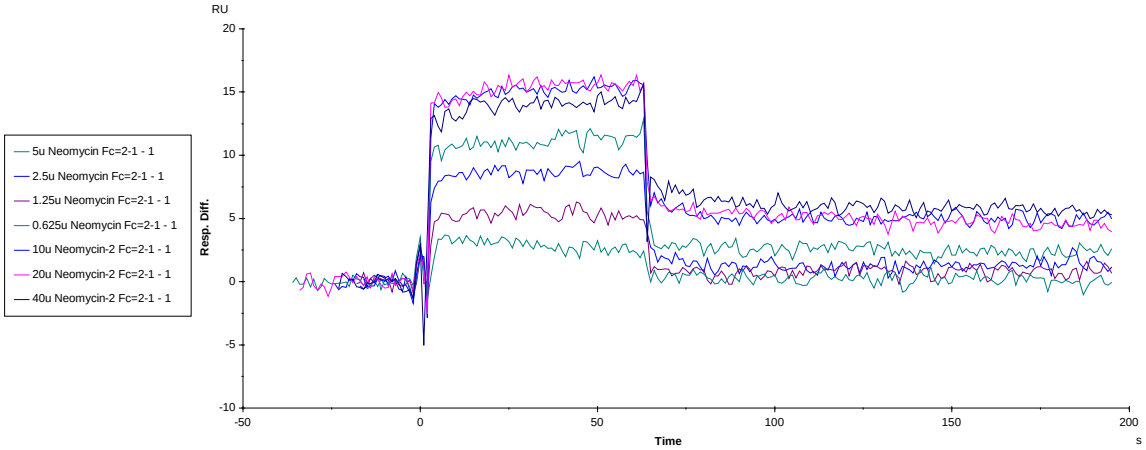

Figure S13. Sensorgrams for binding of neomycin to HIV-1 FSS RNA.

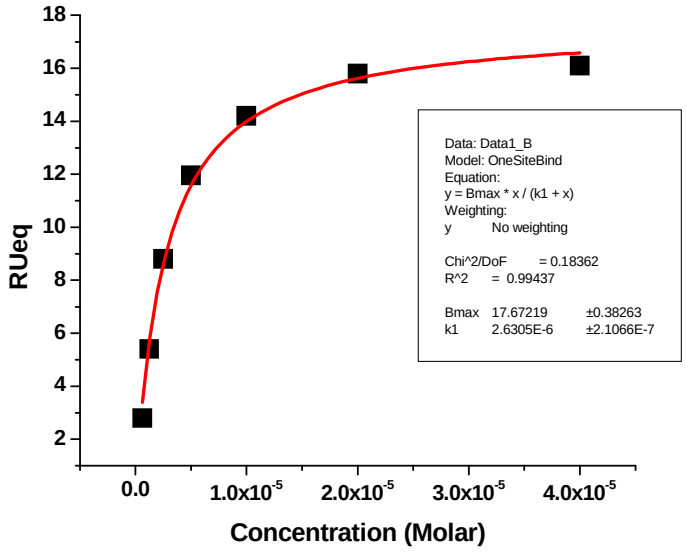

Figure S14. Steady-state binding analysis of SPR data for neomycin binding the HIV-1 FSS RNA.

Dynamic Light Scattering Measurements for compounds 9-11:

To rule out non-specific binding of ligands to the HIV-1 FSS RNA by aggregation, dynamic light scattering (DLS) studies were performed. Dynamic light scattering (DLS) data were collected on a DynaPro 801 Molecular Sizing Instrument (Protein Solutions Inc). All measurements were recorded at 22 °C. The compounds were dissolved in 1X PBS buffer (pH 7.2). Pre-filtered samples were taken into a 12 µL cell and illuminated by a 25 mW laser at 750 nm. The detector angle was 90°. The hydrodynamic radius (H_r) was calculated using the dynamic software package version 4.0. Ten repeat measurements were performed on each sample and the data was filtered based on sum of squares (SOS) and baseline error calculations. Each reported intensity value is an average of three or more measurements.

Table S2. Dynamic light scattering measurements for the all-carbon compounds. All measurements were carried out in 1X PBS buffer (pH 7.2). The hydrodynamic radius (H_r) values obtained for **9, 10** and **11** are approximate as the low intensity in the case of these compounds is a significant source of error.

.

Compound	Concentration (µM)	H_r by regularization (nm)	H_r by Dynals (nm)	Intensity (kcps)
1X PBS Buffer	-	No particles	No particles	6.9 ± 0.51
Congo Red	750	69.25	52.80	242 ± 10
Congo Red with TX-100 (0.01%)	750	40.72	34.50	190 ± 24
9	1000	0.73	0.50	7.55 ± 0.41
10	1000	0.51	0.43	7.34 ± 0.46
11	1000	0.83	0.94	10.14 ± 1.66

Congo Red is a dye known to form aggregates,[3] and hence was used as a positive control to study the aggregation of all-carbon ligands. The dye formed aggregates at a concentration of 750 µM in the 1X PBS buffer with a hydrodynamic radius of 53 nm. The formation of aggregates was evident from the high counts per seconds (kcps) compared to the buffer. Also, there was decay in the autocorrelation function observed over 10 to 10,000 µs scale. On the contrary, compounds **9, 10** and **11** at 1 mM concentration in 1X PBS buffer, did not show any aggregation as they yielded very low intensities (kcps) close to the value of the PBS buffer and an autocorrelation function lacking a well-defined decay over time.

[3] McGovern, S. L., Helfand, B. T., Feng, B., Shoichet, B. K. A specific mechanism of nonspecific inhibition. *J. Med. Chem*. **2003**, 46, 4265-4272.